A NUMERICAL MODELLING AND OBSERVATIONAL EFFORT TO DEVELOP THE CAPABILITY TO PREDICT THE CURRENTS IN THE GULF OF MEXICO FOR USE IN POLLUTANT TRAJECTORY COMPUTATION

A FINAL REPORT SUBMITTED TO
THE BUREAU OF LAND MANAGEMENT
UNDER
BLM INTERAGENCY AGREEMENT 08550-IA5-26

A GUIDE TO A GENERAL CIRCULATION MODEL OF THE GULF OF MEXICO

May 1976

David W. Behringer
Robert L. Molinari
John F. Festa

National Oceanic and Atmospheric Administration
Atlantic Oceanographic and Meteorological Laboratories
Miami, Florida

EXECUTIVE SUMMARY

The Atlantic Oceanographic and Meteorological Laboratories of the National Oceanic and Atmospheric Administration have completed the first year of a proposed two-year study for the Bureau of Land Management "to develop the capability to predict the currents in the Gulf of Mexico for use in pollutant trajectory computation". The objectives of the study were:

(1) to modify an existing numerical model for application in the Gulf of Mexico;

(2) to evaluate the ability of the model to simulate the Gulf circulation using various types and distributions of data as input information; and

(3) to describe the Gulf of Mexico circulation using the results of the model.

The formulation of the numerical model and the modifications made are given in the portion of this report entitled "A Guide to a General Circulation Model of the Gulf of Mexico". The data used by the model as interior and boundary conditions were obtained from the National Oceanographic Data Center, and from cruises conducted as part of the present study. The manipulations used to put the data into a form suitable for input to the model are described in the section called "Model Studies of the Circulation in the Gulf of Mexico".

The ability of the numerical model to simulate the observed circulation is demonstrated through a series of comparisons of its solutions with solutions from a geostrophic model. These comparisons are made over a wide range of input and boundary conditions. Therefore, the use of the numerical model results to describe the currents of the region is justified.

The circulation of the Gulf of Mexico at monthly increments is simulated by both models. The solutions are consistent with the results of previous investigations in regard to such large-scale features as the Loop Current, and a gyre in the western Gulf. In addition, the temporal variability of circulation features on the west Florida, MAFLA, and Texas-Louisiana Shelfs are described in detail for the first time.

The results of the monthly increment experiments suggest that significant interactions may occur between the sub-regions of the Gulf. The study of these interactions through the use of the model in a prognostic mode is planned for the second year of the program. The effect of the wind field, and other motion-inducing factors on the circulation will also be evaluated. In addition, the ability of the numerical model to perform in a prognostic mode with input of real-time data is to be tested. The refinement of the data handling techniques is a necessary step in order to meet these objectives, and is planned for next year's effort.

TABLE OF CONTENTS

TABLE OF CONTENTS

1. Introduction

In this guide a numerical model is described which simulates the three dimensional circulation of water in the Gulf of Mexico. It has been adapted from the general oceanic circulation model developed by Bryan (1969) and his co-workers at the Geophysical Fluid Dynamics Laboratory of NOAA.

The similarity between the Gulf of Mexico and the major oceans, and therefore the reasons for studying the Gulf with an ocean model, is not immediately obvious. For instance, the Gulf is relatively small compared to the ocean basins (it has a surface area of only about 2% of that of the North Atlantic Ocean) and unlike the major basins, the Gulf has two narrow ports through which considerable flux of mass occurs. However, the Gulf is very similar to the oceans in several important respects. The Gulf is deep, and it is vertically stratified in density. There is an intense current in the east, which later joins the Gulf Stream and, in the western basin, there appears to be a closed wind-driven circulation with an intensification of the flow toward the west (Sturges and Blaha, 1976).

These similarities between the Gulf of Mexico and the oceans suggest that the Gulf, despite its size and other differences, can be properly represented by an ocean model. In fact, as we shall see, the size of the Gulf will be a particular advantage in the model.

We will begin with a brief overview of the development of circulation models. This discussion will introduce some of the features of ocean dynamics which a successful model must include and point out a potential source of error in the parameterization of friction.

a. Circulation Theory

Traditionally, circulation theory has developed along two separate lines, one describing the wind-driven circulation and the other the thermohaline circulation. The separation is artificial but it was necessary because of the difficulty in solving the combined problem. We will first consider the theory aimed at understanding the large wind-driven gyres which dominate the surface circulation of the oceans.

Using a simple frictionless, wind-driven model, Sverdrup (1947) demonstrated the influence of the combined effect of the rotation of the earth and the curvature of the surface of the earth in the dynamics of the interior of the ocean basins (the so-called β-effect). This important result established the relationship between the meridional transport of water and the local wind stress. The following year, Stommel (1948) showed, using a wind-driven, frictional model, that the intensification of the currents along the western boundary of the oceans was also the direct consequence of the β-effect. Stommel's results represented the first satisfactory explanation of the Gulf Stream phenomenon.

Munk (1950) produced the first complete theory of a frictional, wind-driven circulation. Using actual wind

observations Munk was able to account for many of the features of the real ocean. However, the theory could not accurately predict the observed strength and width of the real western boundary currents. The theoretical currents were too weak and too wide.

Part of the difficulty seems to be that the Munk model is linear, i.e. it neglects the nonlinear inertial effects of the self-advection of the velocity field. Using a model with a purely inertial western boundary region Morgan (1956) was able to predict a more accurate width for the Gulf Stream than that given by Munk (1950). Morgan and others (Charney 1955; Carrier and Robinson 1962) clearly demonstrated the importance of inertial effects in the intense western boundary currents. However, the mathematical difficulties involved in finding analytical solutions to non-linear problems prevented further study of models with a realistic mixture of inertial and frictional effects.

These difficulties were overcome as a result of the growth in the use of high-speed computers and the development of numerical models. Nonlinear problems, formerly intractable, could now be solved. In one such study Veronis (1966) showed that a decrease in the effect of friction in a fully non-linear model resulted in an increase in the transport of the western boundary current. However, the model cannot predict an upper bound for the transport;

the transport continues to increase indefinitely as the friction is decreased further. In a similar study, Bryan (1963) compared his numerical non-linear solutions to the corresponding linear solutions of Munk (1950). The non-linear solutions consistently showed a greater transport in the western boundary currents.

In addition, both studies demonstrated that even in a highly inertial model the magnitude of the currents is ultimately determined by the strength of the frictional effects. Therefore, it is important to parameterize the model friction correctly. Unfortunately, no one has been able to formulate an accurate parameterization of friction and thus the treatment of friction remains a potential source of error in circulation models.

The other main line of circulation theory attempts to explain the thermohaline circulation which is driven by the differential heating, precipitation, and evaporation at the surface of the ocean. One of the most interesting of these theories is based on a simple model devised by Stommel (1958); (see also Stommel, 1965). By postulating a localized sinking of water at high latitudes and a broad, slow, upward movement of water over the central ocean basin, Stommel was able to deduce the deep circulation pattern: a broad slow poleward drift in the interior of the ocean with return flow confined to a sub-surface western boundary current. This prediction of a counterflow under the Gulf Stream has since been confirmed by observations (Warren, 1971).

The mathematical theory of the thermohaline circulation is not as complete as the theory of the wind-driven circulation. However, partial solutions for the interior of the oceans propose a balance between the upward advection of heat and the downward diffusion of heat due to turbulent mixing. The solutions give good quantitative predictions of the depth and thickness of the thermocline and the magnitudes of the vertical velocity and eddy diffusion (Veronis, 1969).

A complete analytical theory which accurately describes the combined wind-driven and thermohaline circulations has not been found. The possibility of solving the combined problem did not occur until the pioneering work of Sarkisyan (1966) and Bryan and Cox (1967) with three-dimensional numerical ocean models designed to be solved by computer.

b. The Numerical Ocean Model of Bryan

We have chosen as a model an adaption of the three dimensional ocean model developed by Bryan (1969). We will discuss qualitatively, but in some detail, the physical principles and assumptions underlying the Bryan model and the modifications we have made to it.

The basis of the model is the set of physical laws governing the motion of a fluid on the rotating spherical earth. For the ocean these laws represent the conservation of mass, the conservation of momentum (Newton's second law of motion), the conservation of internal energy (the

second law of thermodynamics), the conservation of salinity and an equation of state which gives the density as a function of pressure, temperature and salinity. The mathematical expression of these laws is a set of partial differential equations which govern the temporal evolution of seven independent field variables: three components of velocity (eastward, northward, vertical), temperature, salinity, pressure, and density.

In order to construct the numerical equivalent to these equations, the model region is first filled with a three-dimensional array of grid points. Then a set of finite-difference equations are constructed which approximate the differential equations at the grid points. The finite-difference equations are algebraic and can be solved on a computer.

The resolution of the numerical model is determined by the distance between grid points. For example, the Gulf of Mexico model with 37,26, and 7 grid points, respectively, in the zonal, meridional, and vertical directions has a uniform horizontal resolution of about 50 kilometers and a variable vertical resolution of 70 to 930 meters. An increase in the number of grid points allows a finer-resolution but also requires more computer memory and time to perform a calculation.

The particular set of equations which are used do not represent the most general form of the physical laws; they

have been simplified by taking advantage of certain characteristics of the ocean. The simplifications are necessary in order to obtain solutions because of reasons to be discussed below. The following are the most important approximations.

1) The ocean is assumed to be a Boussinesq fluid. This assumption is based on the fact that the density of the ocean differs only slightly from a reference state in which entropy and salinity are constant and there is no motion. Using this fact, a simple analysis (Phillips, 1966) shows that, to a good approximation, the ocean is incompressible and the variation of density is only important when it affects the buoyancy of the water.

2) The ocean is assumed to be in hydrostatic balance. This means that the vertical balance of forces differs only slightly from a reference state of no motion. Thus, the conservation equation for the vertical component of momentum is replaced by the so-called hydrostatic balance between the vertical gradient of pressure and the buoyancy force per unit volume. Vertical accelerations of the water are neglected. Although upwelling and downwelling are generally not affected by the assumption, rapid unstable, convective sinking is precluded. This difficulty is corrected by parameterizing convection so that when dense water overlies less dense water it is instantaneously mixed downward until neutral static stability is re-established. A

discussion of the hydrostatic approximation can be found in Fofonoff (1962).

3) The surface of the ocean does not coincide with the geoid even if wind waves and tidal fluctuations are neglected. Variations in the elevation of the surface are an important part of the dynamics of the circulation. However, for computational reasons the surface of the model ocean is fitted with a rigid lid. Under the rigid lid approximation the relative elevation of the surface is replaced by an equivalent surface pressure. The approximation filters out surface gravity waves and slightly distorts other time-dependent motions. The mean circulation is not significantly affected. Clearly, this assumption should not be used in studies in which surface gravity waves are important these would include tidal studies (Hendershott and Munk, 1970), storm surge problems (Reid and Bodine, 1968), and estuarine studies (Leendertse, 1970).

4) The equations which are used govern only the large-scale motion. Formally these equations are derived by an averaging procedure from the more general equations representing all scales of motion (Phillips, 1969; Monin and Yaglom, 1971). If each of the field variables is separated into large-scale and small-scale parts, then the averaged equations can be expressed entirely in terms of the large-scale variables, with the exception of one term in each of the momentum, heat, and salinity equations, which represents the net effect of all the small-scale variability. In a numeric

model the small-scale variations are those with scales less than the distance between grid points. For convenience, all of the unresolved small-scale motions are called eddies. Because the eddy effects are not resolved they must be parameterized where they appear in the averaged equations. By analogy with the theory of turbulence, it might be assumed that the net effect of all eddy processes was to enhance the diffusion of momentum, heat and salinity. Based on this assumption, the model parameterizes the eddy fluxes by the negative gradient of the appropriate large-scale variable multiplied by a constant, positive eddy coefficient.

Although it is reasonable to use a positive eddy coefficient over most of the ocean, a constant eddy coefficient is probably not justified. Unfortunately, until our understanding of eddy processes is greatly improved, the use of a more sophisticated parameterization is also not warranted. The size of the coefficient required for a successful computation is determined by the resolution of the model; as the resolution becomes coarser the coefficient must be made larger. In fact, the coefficient can readily become too large and mask important inertial effects. Clearly, the finer resolution possible in a small basin, such as the Gulf of Mexico, provides a distinct advantage in this regard.

5) The model assumes that, over most of the basin, the frictional drag of the flow on the bottom is negligible. This is a reasonable assumption for deep water where the

vigorous wind-driven circulation is confined to the surface layers. However, in regions where strong currents extend to the bottom, the assumption breaks down. Therefore, a simple bottom drag has been included, but it is applied only in the shallowest parts of the model.

If the model were to be used in a region which is entirely on the continental shelf, it would be necessary to modify it to include bottom drag everywhere. (For other approaches to shelf modeling see Peng and Hsueh (1974) and Galt (1975)).

With the exception of the shallow water bottom drag, all of the above approximations are included in the basic Bryan model. The only changes specifically needed to adapt the Bryan model to the Gulf of Mexico were modifications to accomodate the open boundaries at the Straits of Yucatan and Florida. Two distinct treatments of the boundary conditions at the Straits have been tried. In one case the model requires information about the direction and vertical structure of the flow at the open boundaries while in the other case the model uses the freer condition that the flow does not change direction at the boundaries. Additionally, in both treatments, the user must specify the total transport of water through the boundaries. A comparison of the results of separate calculations using these different treatments at the boundaries shows only slight differences in the interior of the model Gulf. This

similarity between the solutions suggests that either boundary method is adequate. A more detailed comparison is made in a later section.

Two distinct types of calculations can be done with Bryan model and in each case the data requirements of the model are different. First, the model can be used as a fully predictive model in which the temperature, salinity and two horizontal components of velocity are determined simultaneously (vertical velocity, density and pressure are completely specified by these four). To make such a calculation, the user must first provide an initial value of temperature, salinity, and horizontal velocity at all grid points of the model. In addition, he must supply at every surface grid point the values of the wind stress, the flux of heat through the surface and the apparent flux of salt through the surface as a result of evaporation and precipitation. The calculation then proceeds step by step simulating the evolution in time of the model ocean subject to the initial conditions and the applied forces. A typical experiment may proceed until an equilibrium state is achieved. An advantage of the fully-predictive method is that if only the equilibrium solution is sought, the details of the initial conditions on temperature, salinity and velocity are unimportant. The disadvantage of the method is that a very lengthy calculation is required to reach equilibrium. For example, in a fully predictive

study of the Indian Ocean, using the Bryan model (Cox, 1970), an approximate equilibrium was reached only after 192 model years of calculation corresponding to 270 hours of computing time on a UNIVAC 1108 computer. The long times are required for the deep temperature and salinity fields to reach equilibrium through vertical diffusion.

The second type of calculation, the diagnostic method, avoids this difficulty. In a diagnostic calculation, the user must supply the model with the same type of initial data and forcing data as in a predictive calculation. However, during the calculation the temperature and salinity fields are held fixed, while the velocity field is allowed to evolve to a steady state. The time required for a diagnostic experiment is considerably less than that for a predictive study. For example, in a diagnostic study of the North Atlantic Ocean, using the Bryan model, a steady state was achieved after only 25 to 30 days of model time (Holland and Hirschman, 1972). The quality of the velocity field determined in a diagnostic study depends strongly on the quality of the temperature and salinity data put into the calculation.

The Bryan model has been used in numerous studies of the ocean circulation by several investigators. The studies have been of two kinds. The first kind attempts to isolate the important physical processes in the ocean circulation.

These experiments idealize the basin geometry and the applied forces. In one example, Bryan and Cox (1968) were able to reproduce the major features of the wind-driven and thermohaline circulations and to confirm some of the earlier results of the simpler, non-linear, one-layer models (Bryan, 1963; Veronis, 1966). Another study examined the effects of geometry and topography in an idealized model of the Antarctic Circumpolar Current (Gill and Bryan, 1971). This latter study also illustrates how careful adjustment of the model parameters allows a closer analogy with the real ocean.

The second kind of experiment attempts to simulate the circulation of actual ocean basins. One of the most successful of these studies was the Indian Ocean model of Cox (1970). Cox was able to model the rapid response of the Somali Current to changes in the Monsoon winds. Also in the second category are diagnostic expermients. Holland and Hirschman (1972) have made a diagnostic calculation for the North Atlantic Ocean. One of their most interesting results was the enhancement of the Gulf Stream transport caused by the interaction of the bottom pressure with variations of the bathymetry. More recently, Cox (1975) has described an ambitious effort to model diagnostically the entire world ocean.

Partial reviews of the work done using the Bryan model can be found in Gill (1971) and Bryan (1975).

All of the calculations we have done so far with the Gulf model have been diagnostic. However, the model has been written to make either type of calculation at the option of the user.

In the following two sections we present a technical discussion of the formulation of the mathematical model and the numerical analog of the mathematical model. Most of the points discussed in the introduction are treated more rigorously in these sections. A section covering the programming and operational procedures used in the model is included. We conclude with a section illustrating the use of the model with sample results from diagnostic calculations in the Gulf of Mexico.

2. Development of the Model

a. Eulerian and Lagrangian Descriptions

There are two equivalent ways to describe fluid motion. In a Lagrangian description the physical properties of the fluid are first associated with individual bits of fluid. The fluid motion is then described in terms of the subsequent positions and properties of the fluid bits. Alternatively, in an Eulerian description, the physical properties are attributed to fixed points within the space occupied by the fluid. The fluid motion is then characterized by changes in the properties at the fixed points. These changes occur as the points are sequentially occupied by different bits of fluid.

Observationally, current drogues or neutrally bouyant floats give Lagrangian information while anchored current meters provide Eulerian measurements.

Following a bit of fluid the rate of change with respect to time, t, of any scalar property, q, is defined as $\frac{dq}{dt}$. The local rate of change of q at a point is, also by definition, $\frac{\partial q}{\partial t}$. The instantaneous difference between the two at a point is given by

$$\frac{\partial q}{\partial t} - \frac{dq}{dt} = \frac{\partial q}{\partial t} - \frac{Dq}{Dt} = -\vec{u}\cdot\vec{\nabla}q \qquad 2.1$$

where $\vec{u}$ is the velocity vector and $\vec{\nabla}$ is the gradient operator. The last term is the rate of increase of q at a point due to advection. The Eulerian derivative, $\frac{Dq}{Dt}$, appears in the Eulerian equations of motion and represents the essential non-linearity of the equations.

Solutions to general circulation problems have only been obtained from the Eulerian description, and thus the model uses this specification. However, for some purposes it may be desirable to infer the Lagrangian behavior from the Eulerian solution. When such a translation is attempted it should be done cautiously.

b. Simplifications to the Basic Equations

The derivation of the basic hydrodynamical equations is discussed in Lamb (1932), and in the text by Neumann and Pierson (1966) and will not be presented here.

The development of the model from the basic equations will be presented using a simple rectangular coordinate system. The final model equations which will be given later are written in the more natural spherical coordinates. The choice of a coordinate system will not essentially alter the development.

The rectangular coordinates (x, y, z), are attached to the rotating earth and oriented so that x points eastward, y northward, and z vertically upward. The corresponding velocity components are (u, v, w). Occasionally, tensor notation will be used. Equations written in this form will use $x_i = (x_1, x_2, x_3)$ in place of (x, y, z) and $u_i = (u_1, u_2, u_3)$ in place of (u, v, w). In this notation equation 2.1 becomes

$$\frac{Dq}{Dt} = \frac{\partial q}{\partial t} + u_j \frac{\partial q}{\partial x_j}$$

$$= \frac{\partial q}{\partial t} + u_1 \frac{\partial q}{\partial x_1} + u_2 \frac{\partial q}{\partial x_2} + u_3 \frac{\partial q}{\partial x_3}$$

where, as shown, the appearance of a subscript twice in a single term implies summation over all three subscript values.

The conservation of momentum is expressed by

$$\rho\frac{\partial u}{\partial t} + \rho(\vec{u}\cdot\vec{\nabla})\vec{u} + \rho\vec{\Omega}X\vec{u} = -\vec{\nabla}p - \rho g\hat{k} + \vec{f}_r, \qquad 2.2$$

where $\vec{u}$ and t are defined above and

ρ = density,

$\vec{\Omega} = (0, 2\omega\cos\phi, 2\omega\sin\phi)$ = rotation vector relative to the local vertical direction,

2ω = twice the angular velocity of the earth ($1.46X10^{-4}$ sec^{-1}),

ϕ = latitude,

p = pressure,

g = apparent gravitational acceleration (980 cm sec^{-2}), and

$\hat{k}$ = unit vector in the vertical direction.

The last term represents the frictional force per unit volume. In tensor notation,

$$f_{ri} = 2\mu\frac{\partial e_{ij}}{\partial x_j}$$

where μ = molecular viscosity, and

$$e_{ij} = \frac{1}{2}\left(\frac{\partial u_i}{\partial x_j} + \frac{\partial u_j}{\partial x_i}\right)$$

is the rate of strain tensor.

The equation for the conservation of mass has the form

$$\frac{\partial\rho}{\partial t} + \vec{\nabla}\cdot(\rho\vec{u}) = 0 . \qquad 2.3$$

Equation 2.3 is also called the continuity equation.

An equation for the internal energy of a fluid can be derived from an equation for the rate of change of entropy (Phillips, 1966). In terms of potential temperature, θ, the equation has the form

$$\rho\frac{\partial\theta}{\partial t} + \rho\vec{u}\cdot\vec{\nabla}\theta = \kappa\nabla^2\theta + \frac{Q}{c_{vs}} \qquad 2.4$$

where k is the coefficient of molecular diffusion for temperature, Q is the rate of generation of heat by friction and c_{vs} is the heat capacity of sea water at constant specific volume and salinity. The last term is negligible.

Sea water is a solution of many salts but it is convenient to represent the concentration of all the salts by a single salinity, s, expressed as the mass of dissolved solids per unit mass of water. The equation for the conservation of salinity is

$$\rho\frac{\partial s}{\partial t} + \rho\vec{u}\cdot\vec{\nabla}s = D\vec{\nabla}\cdot(\rho\vec{\nabla}s) \qquad 2.5$$

where D, is the coefficient of molecular diffusion for salinity.

Finally, the equation of state for density can be expressed as a function of the three other thermodynamic variables, pressure, potential temperature, and salinity:

$$\rho = \rho(p,\theta,s) \qquad 2.6$$

There is no simple analytic form for this equation; Fofonoff(1962a) reviews a number of empirical approximations.

Together with appropriate initial conditions and boundary conditions equations 2.2 through 2.6 represent a complete description of the dynamics of the ocean. However, before the equations can be solved they must first be simplified.

The Boussinesq approximation is discussed in detail by Phillips (1966) and will only be given in outline here. To a good approximation, the ocean differs only slightly from an isentropic state so that $dp \approx c^2 d\rho$ where c is the speed of sound in sea-water. In addition, variations in pressure are mainly due to variations in depth so that $dp \approx -\rho g\, dz$.

Combining these approximations, the rate of change of density is

$$\frac{d\rho}{dt} = \frac{1}{c^2}\frac{dp}{dt} = -\frac{\rho g}{c^2} w \qquad 2.7$$

Using equation 2.3 then

$$\vec{\nabla}\cdot\vec{u} = \frac{\partial u}{\partial x} + \frac{\partial v}{\partial y} + \frac{\partial w}{\partial z} = \frac{g}{c^2} w \qquad 2.8$$

where the ratio c^2/g is usually referred to as the scale depth D. In the ocean, D~200 km while the vertical scale for the variation of the vertical velocity is at most the depth of the ocean, about 5 km. Thus, the right hand side of equation 2.8 is negligible compared to the third term on the left hand side and the equation can be written, to a good approximation as

$$\vec{\nabla}\cdot\vec{u} = 0 \,. \qquad 2.9$$

Equation 2.9 expresses the incompressibility condition and it is used in place of the continuity equation. Again because the pressure is primarily a function of depth, the variations in density are only important when multiplied by the gravitational acceleration. Using this last part of the Boussinesq approximation and the incompressibility condition the momentum equation becomes

$$\rho_o \frac{\partial \vec{u}}{\partial t} + \rho_o (\vec{u}\cdot\vec{\nabla})\vec{u} + \rho_o \vec{\Omega}\times\vec{u} = -\vec{\nabla}p - \rho g\hat{k} + \mu\nabla^2\vec{u} \quad . \qquad 2.10$$

The Boussinesq approximation is good for all oceanic motions with the exception of the propagation of sound waves. However, filtering out the acoustic waves will not affect the overall dynamics of the model equations.

The oceanic circulation is characterized by a great range of spatial and temporal scales. The shortest scales include the apparently random motion associated with irregular wave fields and turbulence. The details of these random motions will vary from one occasion to another even though the average circulation and the observable conditions which affect the motion do not change. In this sense, only the average motion is predictable theoretically. Consequently, the equations of motion as they now stand are not directly applicable; they must first be averaged in an appropriate-way. Usually the average is defined as an ensemble average, taken over a large number of possible solutions to the equations for which the observable initial and boundary conditions are the same.

Formally, the procedure involves separating each variable into averaged and fluctuating parts. Thus, for example,

$$u = \bar{u} + u' \qquad 2.11$$

where the barred letter indicates an averaged quantity and the primed letter indicates a fluctuating quantity. If an overbar denotes the averaging procedure, then

$$\overline{u'} = 0.$$

In order to obtain an expression for the conservation of the average momentum a substitution like that in equation 2.11 is made for each of the variables in equation 2.10. Then, averaging the resulting expression gives

$$\rho_o \frac{\partial \vec{\bar{u}}}{\partial t} + \rho_o (\vec{\bar{u}} \cdot \vec{\nabla}) \vec{\bar{u}} + \rho_o \vec{\Omega} \times \vec{\bar{u}} = -\vec{\nabla}\bar{p} - \bar{\rho} g k + \mu \nabla^2 \vec{\bar{u}} + \vec{R} \qquad 2.12$$

In tensor notation, the last term is written as

$$R_i = \frac{\partial \tau}{\partial x_j} ij$$

where $\tau_{ij} = -\rho_o \overline{u_i' u_j'}$ is the so-called Reynolds stress. The Reynolds stress can be interpreted as a flux of momentum due to the fluctuatng part of the velocity field. Except for the Reynolds stress term the averaged flow obeys an equation identical in form to the equation for the total flow.

The same procedure leads to the averaged equations for the incompressibility condition,

$$\vec{\nabla} \cdot \vec{\bar{u}} = 0 \ , \qquad 2.13$$

the conservation of potential temperature,

$$\rho_o \frac{\partial \bar{\theta}}{\partial t} + \rho_o \vec{\bar{u}} \cdot \vec{\nabla} \bar{\theta} = \kappa \nabla^2 \bar{\theta} + \vec{\nabla} \cdot \vec{H} , \qquad 2.14$$

and the conservation of salinity,

$$\rho_o \frac{\partial \bar{s}}{\partial t} + \rho_o \vec{\bar{u}} \cdot \vec{\nabla} \bar{s} = \rho_o D \nabla^2 \bar{s} + \vec{\nabla} \cdot \vec{N} . \qquad 2.15$$

In equations 2.14 and 2.15 $\vec{H} = -\rho_o \overline{\vec{u}'\theta'}$ and $\vec{N} = -\rho_o \overline{\vec{u}'s'}$ are, respectively, the flux of potential temperature and the flux of salinity due to the fluctuating motion. The generation of heat by mechanical friction has been neglected in equation 2.14.

The problem remains to express the fluxes τ_{ij}, $\vec{H}$, and $\vec{N}$, in terms of the averaged quantities. Usually, the net effect of these terms is assumed to be dissipative (Fofonoff,1962b). Thus, by analogy to molecular friction and molecular diffusion,

$$\tau_{ij} = \begin{cases} A_m \frac{\partial \bar{u}_i}{\partial x_j} , & j=1,2 \\ A_v \frac{\partial \bar{u}_i}{\partial x_j} , & j=3 \end{cases} , \qquad 2.16$$

$$\vec{H} = A_H \vec{\nabla}_H \bar{\theta} + \eta \frac{\partial \bar{\theta}}{\partial z} \hat{k} , \qquad 2.17$$

and

$$\vec{N} = A_H \vec{\nabla}_H \bar{S} + \eta \frac{\partial \bar{S}}{\partial z} \hat{k} \quad , \qquad 2.18$$

where $\vec{\nabla}_H = \frac{\partial}{\partial x} \hat{i} + \frac{\partial}{\partial y} \hat{j}$ is the horizontal gradient operator, A_m and A_v are the constant horizontal and vertical eddy viscosity coefficients, respectively, and A_H and η are the constant horizontal and vertical eddy diffusion coefficients.

The difficulty involved in using simple approximations such as those in equations 2.16, 2.17, and 2.18 is that they must account for the effects of a great variety of small scale motions. It is not likely that proper eddy coefficients would be constant over an entire ocean. In fact, there is even some evidence for a negative viscosity in some localities of the ocean (Webster, 1965). Nevertheless, a more sophisticated treatment of the eddy processes cannot be justified until there is a much better understanding of the small scale motions.

The remaining approximations are accomplished by comparing the relative magnitudes of the terms in equations 2.12 through 2.15 and retaining only the dominant terms. The comparison is made in the following manner.

The ocean does not differ greatly from a reference ocean which is isentropic and static. For the reference ocean the conservation of momentum equation is replaced by the hydrostatic equation:

$$\frac{\partial p_r}{\partial z} = -g\rho_r \qquad 2.19$$

where p_r and ρ_r are, respectively, the pressure and density for the reference ocean. Substracting equation 2.19 from equation 2.12 gives

$$\frac{\partial \vec{u}}{\partial t} + (\vec{u}\cdot\vec{\nabla})\vec{u} + \vec{\Omega}\times\vec{u} = -\frac{1}{\rho_o}\vec{\nabla} p - b\hat{k} + \frac{\mu}{\rho_o}\nabla^2\vec{u} + \frac{A_m}{\rho_o}\nabla_H^2\vec{u} + \frac{A_v}{\rho_o}\frac{\partial^2\vec{u}}{\partial z^2} \qquad 2.20$$

where $p = \bar{p} - p_r$ and $b = \frac{\bar{\rho} - \rho_r}{\rho_o} g$ is the buoyancy force per unit volume.

Equation 2.20 can be put into dimensionless form with the following substitutions:

$$\begin{aligned} (x,y) &= L(\tilde{x},\tilde{y}) \\ z &= H\,\tilde{z} \\ t &= L/V_o\,\tilde{t} \\ (\bar{u},\bar{v}) &= V_o(\tilde{u},\tilde{v}) \\ \bar{w} &= V_o H/L\,\tilde{w} \\ 2\omega &= f \\ p &= \Delta P\,\tilde{p} \\ b &= g'\tilde{b} = \frac{\Delta\rho}{\rho} g\tilde{b} \end{aligned} \qquad 2.21$$

where each term on the right consists of a constant coefficient multiplying a dimensionless variable (indicated by a tilde,~) which has an order of magnitude of unity. H and L are the vertical and horizontal length scales, respectively. V_o is a characteristic velocity scale and the scaling for $\bar{w}$ is derived from the continuity equation. Finally, ΔP and $\Delta\rho$ are the magnitudes of the pressure and density variations.

Ocean currents are slow enough that the vertical pressure gradient is nearly balanced by the buoyancy force. Thus, the proper scaling for ΔP is given by $\Delta P/H = \rho_o g'$. Furthermore, the horizontal pressure gradients are primarily balanced by the Coriolis forces. This approximate balance is expressed by choosing $V_o = \Delta P/\rho_o fL$.

Using the substitutions in 2.21 and writing equation 2.20 in component form gives

$$R_o\left(\frac{\partial u}{\partial t} + \vec{u}\cdot\vec{\nabla}u\right) + \frac{H}{L} w \cos\phi - v \sin\phi =$$

$$- \frac{\partial p}{\partial x} + \frac{R_o}{R_e}\left\{\nabla_H^2 u + \left(\frac{L}{H}\right)^2 \frac{\partial^2 u}{\partial z^2}\right\} + E_H \nabla_H^2 u + E_v \frac{\partial^2 u}{\partial z^2} \qquad 2.22$$

$$R_o\left(\frac{\partial v}{\partial t} + \vec{u}\cdot\vec{\nabla}v\right) + u \sin\phi - \frac{H}{L} w \cos\phi =$$

$$- \frac{\partial p}{\partial x} + \frac{R_o}{R_e}\left\{\nabla_H^2 v + \left(\frac{L}{H}\right)^2 \frac{\partial^2 v}{\partial z^2}\right\} + E_H \nabla_H^2 v + E_v \frac{\partial^2 v}{\partial z^2} \qquad 2.23$$

$$F_r\left(\frac{H}{L}\right)^2\left(\frac{\partial w}{\partial t} + \vec{u}\cdot\nabla w\right) - \frac{fV_o}{g'} u \cos\phi =$$

$$- \frac{\partial p}{\partial z} - b + \frac{F_r}{R_e}\left(\frac{H}{L}\right)^2\left\{\nabla_H^2 w + \left(\frac{L}{H}\right)^2 \frac{\partial^2 w}{\partial z^2}\right\} + \frac{F_r}{R_o}\left(\frac{H}{L}\right)^2\left\{E_H \nabla_H^2 w + E_v \frac{\partial^2 w}{\partial z^2}\right\} \qquad 2.24$$

where

$R_o = \frac{V_o}{fL}$, the Rossby number,

$R_e = \frac{\rho_o V_o L}{\mu}$, the Reynolds number,

$E_H = \frac{Am}{\rho_o f L^2}$, the horizontal Ekman number,

$E_v = \frac{Av^2}{\rho_o f H^2}$, the vertical Ekman number,

$F_r = \frac{V_o}{g' H}$, the internal Froude number.

In equations 2.22 through 2.24 the pressure, Coriolis, and buoyancy terms have a magnitude of unity. The magnitude of the remaining terms can be determined by evaluating the coefficients R_o, R_e, E_h, E_v, F_r, and (H/L).

Consider the Rossby number first. Suppose the magnitude of a particular current is 100 cm/sec and it has a horizontal length scale of variation of 100 km. Then at mid-latitudes ($f \simeq 10^{-4}$) the Rossby number is about 0.1. Thus, if the current speed exceeds 100 cm/sec or the length scale of the current is less than 100 km the Rossby number will approach unity and the non-linear terms will begin to match the Coriolis and pressure terms in 2.22 and 2.23.

The Ekman numbers will be nearly unity only for short length scales. Thus, if $Am = 10^8$ cm^2 sec^{-1}, the horizontal Ekman number increases from .01 to 1 as the length scale decreases from 100 km to 10 km. Simarily, if $Av = 1$ cm^2 sec^{-1}, the vertical Ekman number will exceed unity only for vertical scales less than 100 meters.

The internal Froude number can also be as large as unity. Since $\Delta\rho/\rho_o \simeq 10^{-3}$ and $g \simeq 10^3$cm sec^{-2}, the Froude number will be 1 for $V_o = 100$ cm/sec and $H = 100$ meters. However, F_r only appears in conjunction with $(H/L)^2$ which is always much less than one.

The Reynolds number only approaches unity for extremely small length scales. Thus, molecular viscosity can always be neglected..

Finally, the remaining coefficients, H/L, and fV_o/g are both much less than unity and the terms in which they appear can be neglected.

The potential temperature and salinity equations can also be put in dimensionless form. Equations 2.14 and 2.15 become

$$\frac{\partial\theta}{\partial t} + \vec{u}\cdot\vec{\nabla}\theta = \frac{1}{P_{e\theta}}\{\nabla_H^2\theta + (\frac{L}{H})^2\frac{\partial^2\theta}{\partial z^2}\} + \frac{1}{P_{eh}}\nabla_H^2\theta + \frac{1}{P_{ev}}(\frac{L}{H})\frac{\partial^2\theta}{\partial z^2} \qquad 2.25$$

$$\frac{\partial s}{\partial t} + \vec{u}\cdot\vec{\nabla}s = \frac{1}{P_{es}}\{\nabla_H^2 s + (\frac{L}{H})^2\frac{\partial^2 s}{\partial z^2}\} + \frac{1}{P_{eh}}\nabla_H^2 s + \frac{1}{P_{ev}}(\frac{L}{H})\frac{\partial^2 s}{\partial z^2} \qquad 2.26$$

where V_o, L and H are defined as before and the coefficients are Peclét numbers given by

$$P_{e\theta} = \frac{\rho_o V_o L}{\kappa}$$

$$P_{es} = \frac{V_o L}{D}$$

$$P_{eh} = \frac{\rho_o V_o L}{A_H}$$

and

$$P_{ev} = \frac{\rho_o V_o H}{\eta}$$

The Peclét numbers for molecular diffusion are analogous to the Reynolds number and like the Reynolds number they are much greater than unity for oceanic scales. Thus the molecular diffusion is always negligible compared to turbulent diffusion.

Finally, if only the terms with magnitudes potentially as large as unity are retained in the dimensionless equations, then a simplified set of governing equations can be written. Furthermore, if the simplified equations are put back into dimensional form and if all the overbars and tildes are omitted, then the equations have the form:

$$\frac{\partial \vec{u}_H}{\partial t} + (\vec{u}\cdot\vec{\nabla})\vec{u}_H + (2\omega \sin\phi)\hat{k}X\vec{u}_H = -\frac{1}{\rho_o}\vec{\nabla}p + \frac{Am}{\rho_o}\nabla_H^2\vec{u}_H + \frac{Av}{\rho_o}\frac{\partial^2 \vec{u}_H}{\partial z^2}, \qquad 2.27$$

$$\frac{\partial p}{\partial z} = -\rho g \quad , \qquad 2.28$$

$$\frac{\partial \theta}{\partial t} + \vec{u}\cdot\vec{\nabla}\theta = A_H\nabla_H^2\theta + n\frac{\partial^2\theta}{\partial z^2} \quad , \qquad 2.29$$

$$\frac{\partial s}{\partial t} + \vec{u}\cdot\vec{\nabla}s = A_H\nabla_H^2 s + n\frac{\partial^2 s}{\partial z^2} \quad , \qquad 2.30$$

and

$$\rho = \rho(p,\theta,s) \quad , \qquad 2.31$$

where the horizontal velocity vector $\vec{u}_H$, has been introduced.

3. Equations of the Model

a. Governing Equations

The model equations are the equations 2.27 through 2.31 expressed in spherical coordinates. The notation used is essentially that of Bryan (1969).

Let

$$\begin{aligned} m &= \sec\phi \quad , \\ n &= \sin\phi \quad , \\ u &= a\lambda_t/m \quad , \\ v &= a\phi_t \quad , \end{aligned} \qquad 3.1$$

where a is the radius of the earth, ϕ is the latitude, λ is the longitude, and t is the time coordinate. The vertical coordinate is z, positive upwards, and the vertical velocity is w. When ϕ, λ, z, and t are used as subscripts, partial differentiation is indicated. The advection operator, L, is defined as

$$L\,q = \frac{m}{a}\{(uq)_\lambda + (vq/m)_\phi\} + (wq)_z \qquad 3.2$$

where q is any scalar quantity. The horizontal momentum equations are

$$u_t + L\,u - 2\omega nv - mnuv/a = -\frac{m}{a}(p/\rho_o)_\lambda + F^\lambda + A_v u_{zz} \qquad 3.3$$

and

$$v_t + L\,v + 2\omega nu + mnuu/a = -\frac{1}{a}(p/\rho_o)_\phi + F^\phi + A_v v_{zz} \qquad 3.4$$

The hydrostatic equation is

$$p_z = -\rho g \qquad 3.5$$

and continuity is expressed by

$$\frac{m}{a}\{u_\lambda + (v/m)_\phi\} + w_z = 0. \qquad 3.6$$

The conservation equations for potential temperature, θ, and salinity, s, are given by

$$\theta_t + L\theta = Q \qquad 3.7$$

$$s_t + Ls = \sigma. \qquad 3.8$$

Finally, the equation or state is represented by

$$\rho = \rho(p,\theta,s) \qquad 3.9$$

The particular equation or state used in the model is based on the empirical Knudsen-Ekman formulation (Fofonoff, 1962a). The effects of turbulent viscosity and diffusion are represented by the terms F^{λ}, F^{ϕ}, Q, and σ. If

$$\nabla_H^2 q = m^2 q_{\lambda\lambda} + m(q_{\phi}/m)_{\phi} \quad , \qquad 3.10$$

then

$$F^{\lambda} = \frac{A_m}{a^2}\{\nabla_H^2 u + (1 - m^2n^2)u - 2nm^2 v_{\lambda}\} \quad , \qquad 3.11$$

$$F^{\phi} = \frac{A_m}{a^2}\{\nabla_H^2 v + (1 - m^2n^2)v + 2nm^2 u_{\lambda}\} \quad , \qquad 3.12$$

$$Q = \frac{A_H}{a^2}\nabla_H^2\theta + n\theta_{zz} \quad , \qquad 3.13$$

$$\sigma = \frac{A_H}{a^2}\nabla_H^2 s + n s_{zz} \quad , \qquad 3.14$$

where A_V and A_m are the constant eddy viscosity coefficients in the horizontal and vertical directions, respectfully, and A_H and n are the constant eddy diffusion coefficients.

The hydrostatic approximation disallows unstable convection. Therefore, a parameterization of convection is included to correct any unstable density stratification which may arise. The details of the method are described in the section on the finite difference approximation to the model equations.

b. Boundary Conditions

At the sea surface

$$\rho_o A_V(u_z, v_z) = (\tau^\lambda, \tau^\phi) \qquad \text{at } z = 0 \qquad 3.15$$
$$w = 0$$

where τ^λ and τ^ϕ, are the zonal and meridional components of the wind stress, respectively. Also,

$$\rho_o \eta\ (\theta_z, s_z) = (F^\theta, F^S) \qquad \text{at } z = 0 \qquad 3.16$$

where F^θ is the heat flux across the surface expressed as a flux of temperature and F^S is the net effect of precipitation less evaporation expressed as a flux of salt (the gain or loss of water in this process is ignored).

The condition that $w = 0$ at $z = 0$ is the rigid-lid approximation. It filters out surface gravity waves and slightly distorts barotropic Rossby waves. As will be seen in a later section, the approximation is vital for efficient computation.

At the bottom of the ocean

$$w = -\left(\frac{u}{a}mh_\lambda + \frac{v}{a}h_\phi\right) \qquad \text{at } z = -h(\lambda,\phi) . \qquad 3.17$$
$$(u_z, v_z) = 0$$

A partial modification to the free-slip condition expressed here is described in the section on test results. Also, the flux of heat through the bottom is ignored;

$$(\theta_z, s_z) = 0 \qquad \text{at } z = -h(\lambda,\phi) . \qquad 3.18$$

At lateral boundaries, which are physically closed by a land mass, the horizontal velocity components and the fluxes of heat and salt vanish. In the model for the Gulf of Mexico there are "open" lateral boundaries at the Straits of Yucatan and Florida. At these boundaries the normal derivatives of u, v, θ, and s are set to zero and the total volume transport through the opening is specified. The transports through the two straits must be equal.

c. Volume Transport Stream Function

The rigid-lid approximation eliminates the displacement of the sea surface. Instead there is an equivalent surface pressure, p_s, at the lid, z = 0. Therefore, integrating the hydrostatic equation with respect to z gives

$$p = p_s + \int_z^0 \rho g \, dz' . \qquad 3.19$$

Equation 3.19 is used to replace p in equations 3.3 and 3.4. Since there is no predictive equation for p_s, it must be eliminated.

Integrating the continuity equation from the ocean floor to the surface gives

$$\{(\int_{-h}^{o} u\, dz)_\lambda + (\frac{1}{m}\int_{-h}^{o} v\, dz)_\phi\} = 0 \,. \qquad 3.20$$

Equation 3.20 allows a transport stream function, Ψ, such that,

$$m\Psi_\lambda = a\int_{-h}^{o} v\, dz$$

and $$\Psi_\phi = -\, a\int_{-h}^{o} u\, dz \qquad 3.21$$

Integrating equations 3.3 and 3.4 from the bottom to the surface, multiplying by a/mh and a/h, respectively, and cross-differentiating to eliminate p_s, gives

$$\begin{aligned}(m\Psi_\lambda/h)_{\lambda t} + (\Psi_\phi/hm)_{\phi t} = &- \Psi_\lambda(2\omega n/h)_\phi + \Psi_\phi(2\omega n/h)_\lambda - \frac{1}{\rho_o}\{(\frac{\tau^\lambda}{mh})_\phi - (\frac{\tau^\phi}{h})_\lambda\} \\ &+ \frac{g}{\rho_o}\{(\frac{1}{mh}\int_{-h}^{o}(\int_{z}^{o}\rho_\lambda dz')\, dz)_\phi - \{\frac{1}{h}\int_{-h}^{o}(\int_{z}^{o}\rho_\phi dz')\, dz)_\lambda\} \\ &+ \{(G^\phi/h)_\lambda - (G^\lambda/mh)_\phi\} \end{aligned} \qquad 3.22$$

where

$$\begin{aligned} G^\lambda &= -\, a\int_{-h}^{o}(Lu - \frac{mn}{a}uv - F^\lambda)\, dz \\ G^\phi &= -\, a\int_{-h}^{o}(Lv + \frac{mn}{a}u - F^\phi)\, dz \end{aligned} \qquad 3.23$$

The vertically averaged velocities are :

$$\bar{u} = \frac{1}{h}\int_{-h}^{0} u\, dz = -\frac{1}{ah}\Psi_{\phi} \quad , \qquad 3.24$$

$$\bar{v} = \frac{1}{h}\int_{-h}^{0} v\, dz = \frac{m}{ah}\Psi_{\lambda} \quad ,$$

where the overbar indicates a vertical average. If the deviations from the average velocities are indicated by $(\hat{u},\hat{v})$, then

$$(u,v) = (\bar{u},\bar{v}) + (\hat{u},\hat{v}) \; . \qquad 3.25$$

The average velocities are predicted by equations 3.22 and 3.24. The $(\hat{u},\hat{v})$ components are determined from equations 3.3 and 3.4. First, the interim components (u',v') are predicted by equations 3.3 and 3.4 with p_s temporarily set to zero. Then

$$(\hat{u},\hat{v}) = (u',v') - (\bar{u}',\bar{v}') \; , \qquad 3.26$$

Equation 3.26 is valid because (u',v') differ from $(\hat{u},\hat{v})$ only by a constant which is independent of z and which is eliminated by substracting out $(\bar{u}',\bar{v}')$.

The boundary condition for equation 3.22 is that Ψ is constant along closed lateral boundaries. In the Gulf model the constant is zero along the coastline of Mexico and the United States and equal to the total transport through the straits along the coastline of Cuba.

4. Finite Difference Equations

a. General Principles

The finite difference equation for any quantity, q, is constructed by approximating the partial derivatives of the differential equation by differences in q between the points of a specified computational grid. It is important to construct the finite difference equations so that momentum, energy and the mean square temperature and salinity will be conserved in the absence of dissipation. Such a formulation will avoid nonlinear computational instabilities and the accumulation of systematic errors in long-term integrations (Arakawa, 1966). Bryan (1969) illustrates the principles involved in the following way.

Let

$$q_t + \vec{\nabla}\cdot(\vec{u}q) = 0 \qquad 4.1$$

$$\vec{\nabla}\cdot\vec{u} = 0 \qquad 4.2$$

where q is any scalar quantity and $\vec{u}$ is the velocity vector. Let the total volume under consideration be divided into N cells, each with a volume of α_i. Integrating equation 4.1 over a cell gives

$$\alpha_i \frac{\partial Q_i}{\partial t} = - \oint q\vec{u}\cdot\hat{n}\, ds \qquad 4.3$$

where Q_i is the average of q for the cell, $\hat{n}$ is the unit vector normal to the cell surface, and $\oint(\,)ds$ indicates integration over the cell surface.

Although other arrangements are possible suppose each face of the cell is a rectangle. Then an approximation to equation 4.3 is

$$\alpha_i \frac{\partial Q_i}{\partial t} = - \sum_{m=1}^{6} q_{im} u_{im} A_{im} \qquad 4.4$$

where u_{im} is the normal velocity and q_{im} is the value of q at the face m and A_{im} is the area of the face m. Similarly the continuity equation becomes

$$\sum_{m=1}^{6} u_{im} A_{im} = 0 \; . \qquad 4.5$$

Next let

$$I_1 = \sum_{i=1}^{N} Q_i \alpha_i \qquad 4.6$$

$$I_2 = \sum_{i=1}^{N} Q_i^2 \alpha_i \qquad 4.7$$

where I_1 and I_2 represent the volume integrals of q and q^2 respectively. The rates of change of the integrals are:

$$\frac{\partial I_1}{\partial t} = - \sum_{i=1}^{N} \left(\sum_{m=1}^{6} q_{im} u_{im} A_{im} \right) \; , \qquad 4.8$$

and

$$\frac{\partial I_2}{\partial t} = -2 \sum_{i=1}^{N} \left(\sum_{m=1}^{6} q_{im} Q_i u_{im} A_{im} \right) \; . \qquad 4.9$$

If there is no net flow out of the whole volume, then $\frac{\partial I_1}{\partial t} = 0$. This is true because, in the interior, adjacent cells contribute equal and opposite terms to the total sum in equation 4.8. The same arguement will not apply to equation 4.9 and, in general, $\frac{\partial I_2}{\partial t}$

does not vanish. However, it will vanish, if the value of q on the face of cell is interpolated according to the formula

$$q_{im} = \frac{1}{2}(Q_i + Q_{im}) \,, \qquad 4.10$$

where Q_{im} is the average value of q in the cell adjacent to the i^{th} cell. If equation 4.10 is substituted into 4.9, then

$$\frac{\partial I_2}{\partial t} = - \sum_{i=1}^{N} \left(Q_i^2 \sum_{m=1}^{6} u_{im} A_{im} + \sum_{m=1}^{6} Q_i Q_{im} u_{im} A_{im} \right) \qquad 4.11$$

The first term on the right is zero by continuity and the second term vanishes by the same cancelling effect as in equation 4.8.

With this formulation the mean value of q and mean square value of q are conserved for the volume as a whole.

b. Finite Difference Equations

The finite difference equations for momentum, potential temperature and salinity presented in this section are conservative in the sense described in section 4a. The formulation and notation is due to Bryan (1969).

Cells with the indices i,j, and k are centered on grid points with the coordinates

$$\lambda_i = \lambda_o + \sum_{i=1}^{i} \Delta\lambda \,, \qquad 4.12$$

$$\phi_j = \phi_o + \sum_{j=1}^{j} \Delta\phi \,, \qquad 4.13$$

$$z_k = - \sum_{k=1}^{k} \Delta_{k'} \,. \qquad 4.14$$

The horizontal velocity components associated with the cells are specified at grid points with integer values,

while temperature, salinity, and the stream function are specified at grid points with indices given by i+1/2, j+1/2 and k. The arrangement of the variables in a horizontal plane is shown in Figure 1.

The vertical velocity points used in the calculation of velocity have the indices i, j and k+1/2, while the vertical velocity points used in the calculation of temperature and salinity have the indices i+1/2, j+1/2, and k+1/2.

The superscripts, $\ell-1, \ell$, and $\ell+1$ are used to indicate the time levels $t-\Delta t$, t, and $t+\Delta t$, respectively. The horizontal grid point separations, $\Delta\lambda$ and $\Delta\phi$, are constant, while the vertical separation, Δ_k, varies. The separation between the k and k+1 points is given by Δ_{k+1} and the thickness the of the k^{th} cell, $\Delta_{k+\frac{1}{2}}$, is determined by

$$\Delta_k = \frac{1}{2}\left(\Delta_{k-\frac{1}{2}} + \Delta_{k+\frac{1}{2}}\right)$$

The lateral boundaries of the model coincide with velocity points; in Figure 1 a boundary can only lie along a broken line. Because of this constraint, it is sometimes useful to imagine the model region to be filled with stacks of boxes, each with a θ,s point located at its center. The depth at a column of θ,s points is determined by the number of boxes stacked at that point. The depth at a column of u,v points is given by the minimum depth at the four surrounding columns of θ,s points.

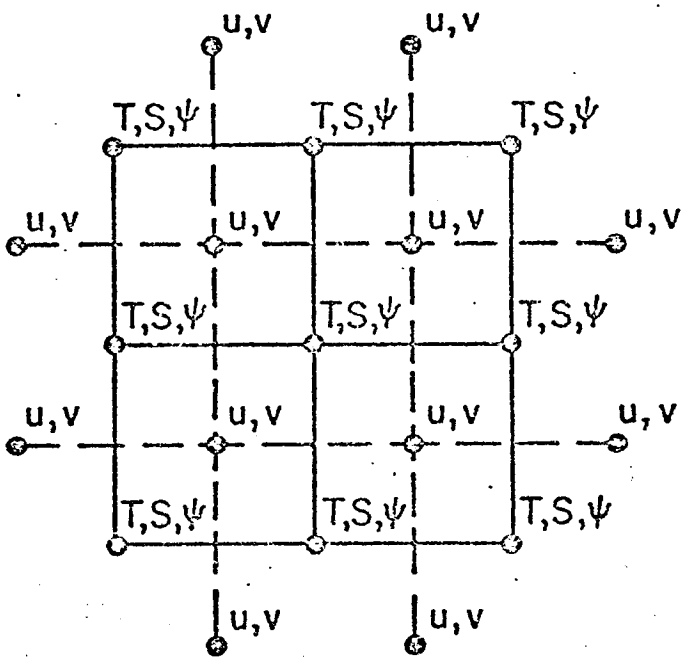

Figure 1. The arrangement of variables in a horizontal plane.

In the finite difference equations which follow it is convenient to use the shorthand notation:

$$\delta_\lambda q = \frac{1}{\Delta\lambda}\left(q_{i+\frac{1}{2}} - q_{i-\frac{1}{2}}\right) , \qquad 4.15$$

and

$$\bar{q}^{\lambda} = \frac{1}{2}\left(q_{i+\frac{1}{2}} + q_{i-\frac{1}{2}}\right) , \qquad 4.16$$

where q is any scalar quantity. When vertical differences are involved

$$\delta_z q = \frac{1}{\Delta_{k+\frac{1}{2}}}\left(q_{k-\frac{1}{2}} - q_{k+\frac{1}{2}}\right) . \qquad 4.17$$

Finally, when time differences are involved

$$\delta_t q = \frac{1}{2\Delta t}\left(q^{\ell+1} - q^{\ell-1}\right) . \qquad 4.18$$

Using this notation, a finite difference analog to the advection operator, L, is

$$L^*(q) = \frac{m}{a}\left\{\delta_\lambda(\bar{u}^{\phi}\bar{q}^{\lambda}) + \delta_\phi(\bar{v}^{\lambda}\bar{q}^{\phi}/m)\right\} + \delta_z(w\bar{q}^{z}) \qquad 4.19$$

where a and m retain the meanings of section 3a. Equation 4.19 is correct only if q is located at a θ,s point.

The conservation of potential temperature can be written in finite difference form as

$$\delta_t\theta = - L^*\theta + \eta\delta_z(\delta_z\theta)^{\ell-1} + \frac{A_H}{a}\left\{m^2\delta_\lambda(\delta_\lambda\theta) + m\delta_\phi\left(\frac{1}{m}\delta_\phi\theta\right)\right\}^{\ell-1} , \qquad 4.20$$

where A_H and η are, respectively, the horizontal and vertical coefficients for eddy diffusion. The indices in equation 4.20 are understood to be i+1/2, j+1/2, k, ℓ except when otherwise specified. The vertical velocity which is used in equa-

tion 4.20 is determined by the continuity equation,

$$L^*(1) = 0 \qquad 4.21$$

and the surface boundary condition, w=0. Finally, note that the advective term is calculated using θ at time t, while the diffusive terms are determined from θ at time $t-\Delta t$.

The equation for the salinity is identical in form to equation 4.20 and it will not be given explicitly here.

It should be pointed out at this time how the model handles unstable convection. First, preliminary values of $\theta^{\ell+1}$ and $s^{\ell+1}$ are predicted for a column of points using equation 4.20 and a similar equation for salinity. Then these values are used in the equation of state to compute the density, $\rho^{*\ell+1}$, referred to surface pressure. The column is then checked for static stability. The column is stable if for every pair of points

$$\rho^{*\ell+1}_k > \rho^{*\ell+1}_{k+1}$$

If the column is stable the calculation proceeds. If the column is unstable, $\theta^{\ell+1}$ and $s^{\ell+1}$ are made uniform over the unstable part of the column by applying an average weighted by the appropriate layer thicknesses. The column is then rechecked for stability. The process will be repeated until the entire column is stable.

The horizontal velocity components, (u,v), are partitioned into a vertically averaged part, $(\bar{u},\bar{v})$, and a baroclinic part, (u',v'), which deviates from the average. Thus,

$$(u,v) = (\bar{u},\bar{v}) + (\hat{u},\hat{v}) \quad . \qquad 4.22$$

The average components are given by the finite difference form of equation 3.24,

$$\bar{u} = -\frac{1}{Ha}\,\delta_{\phi}(\bar{\psi}^{\lambda}) \qquad 4.23$$

$$\bar{v} = \frac{m}{Ha}\,\delta_{\lambda}(\bar{\psi}^{\phi}) \qquad 4.24$$

where ψ is the stream function and H is the depth at the u,v point. The components $(\hat{u},\hat{v})$ obey the conditions

$$\sum_{k'=1}^{kz} \hat{u}\Delta_{k'+\frac{1}{2}} = 0 \qquad 4.25$$

and

$$\sum_{k'=1}^{kz} \hat{v}\Delta_{k'+\frac{1}{2}} = 0 \qquad 4.26$$

where kz is the total number of levels in the column.

A second advection operator can be defined in terms of these variables;

$$L^{**}(q) = \frac{m}{a}\{\delta_{\lambda}(U\bar{q}^{\lambda}) + \delta_{\phi}(\frac{1}{m}V\bar{q}^{\phi})\} + \delta_{z}(w\bar{q}^{z}) \quad . \qquad 4.27$$

Here

$$U = \bar{u}^{\lambda} - \frac{1}{Ha}\,\delta_{\phi}\Psi \qquad 4.28$$

and

$$V = \bar{v}^{\phi} + \frac{m}{Ha}\,\delta_{\lambda}\Psi \qquad 4.29$$

where H is now the least of the two depths for the pair of columns of u,v points used in the interpolation.

As was explained in section 3a the interim velocity components (u',v') are first calculated from the momentum equations in which the surface pressure is set to zero. Then the components $(\hat{u},\hat{v})$ are calculated using

the rules

$$\hat{u}_k = u'_k - \frac{1}{H} \sum_{k'=1}^{kz} u'_{k'} \Delta_{k'+\frac{1}{2}} \qquad 4.30$$

and

$$\hat{v}_k = v'_k - \frac{1}{H} \sum_{k'=1}^{kz} v'_{k'} \Delta_{k'+\frac{1}{2}} \qquad 4.31$$

The equations for u' and v' are

$$u' = u^{\ell-1} + 2\Delta t \, R^{\lambda} \qquad 4.32$$

and

$$v' = v^{\ell-1} + 2\Delta t \, R^{\phi} \qquad 4.33$$

Here,

$$\begin{aligned} R^{\lambda} = &- L^{**}(u) + \frac{mn}{a} uv + 2\omega nv - \frac{m}{a\rho_o} \delta_{\lambda}(\bar{p}^{*\phi}) \\ &+ A_v \delta_z (\delta_z u)^{\ell-1} + \frac{Am}{a^2} \{m^2 \delta_{\lambda}(\delta_{\lambda} u) + m\delta_{\phi}(\tfrac{1}{m}\delta_{\phi} u) \\ &+ (1 - n^2m^2)u - 2nm^2\delta_{\lambda} v\}^{\ell-1} \end{aligned} \qquad 4.34$$

and

$$\begin{aligned} R^{\phi} = &- L^{**}(v) - \frac{mn}{a} u^2 - 2\omega nu - \frac{1}{a\rho_o} \delta_{\phi}(\bar{p}^{*\lambda}) \\ &+ A_v \delta_z (\delta_z v)^{\ell-1} + \frac{Am}{a^2} \{m^2 \delta_{\lambda}(\delta_{\lambda} v) + m\delta_{\phi}(\tfrac{1}{m}\delta_{\phi} v) \\ &+ (1 - n^2m^2)v + 2nm^2\delta_{\lambda} u\}^{\ell-1} \end{aligned} \qquad 4.35$$

where

$$p^*_k = g \{(\rho_1 \Delta_1) + \frac{1}{2} \sum_{k'}^{kz} (\rho_{k'} + \rho_{k'-1}) \Delta_{k'}\} \quad . \qquad 4.36$$

The vertical velocities which are required in equations 4.34 and 4.35 are computed from the continuity equation,

$$L^{**}(1) = 0 \qquad 4.37$$

and the surface boundary condition, w=0.

The finite difference vorticity equation for the stream function is derived by a procedure exactly analogus to that in section 3. The resulting equation is

$$\frac{m}{a}\{\delta_\lambda(\frac{\bar{m}}{a\bar{H}^\phi}\,\delta_\lambda D) + \delta_\phi(\frac{1}{am\bar{H}^\lambda}\,\delta_\phi D)\} =$$

$$\frac{4\omega m\Delta t}{a}\{\delta_\lambda(\overline{\frac{n}{a\bar{H}}(\delta_\phi\bar{\Psi}^\lambda)})^\phi - \delta_\phi(\overline{\frac{n}{a\bar{H}}(\delta_\lambda\bar{\Psi}^\phi)})^\lambda\}^{\ell-1}$$

$$+\frac{2\Delta tm}{a}\{\delta_\lambda(\overline{\frac{1}{\bar{H}}\sum_{k'}^{k''}R^\phi\Delta_{k+\frac{1}{2}}})^\phi - \delta_\phi(\overline{\frac{1}{\bar{H}}\sum_{k'}^{k''}R^\lambda\Delta_{k+\frac{1}{2}}})^\lambda\} \qquad 4.38$$

where $D = \Psi^{\ell+1} - \Psi^{\ell-1}$. Equation 4.38 is in the form of a Poisson equation for D. The left hand side of the equation is a 5-point approximation to the Laplacian. The equation is solved by successive over relaxation (SOR) (Forsythe and Wasow, 1960) More efficient methods for solving Poisson's equation exist but SOR allows the most generality in the shape of the boundary.

The equation of state takes advantage of the discreet layering of the model. In fact, there are separate equations for each layer of the model. Each equation represents a least squares fit of a polynomial with ten terms to the empirical Knudsen-Ekman formula for density (Fofonoff, 1962a). Because each equation is applied only at one level , pressure does not appear explicitly. Each least squares fit is made to a range of values of potential temperature and salinity appropriate to the particular layer. The polynomial has the form:

$$(\rho_k - 1)X10^3 = C_{k1} + C_{k2}\theta_k^* + C_{k3}s_k^* + C_{k4}\theta_k^{*2}$$
$$+ C_{k5}s_k^{*2} + C_{k6}s_k^*\theta_k^* + C_{k7}\theta_k^{*3}$$
$$+ C_{k8}\theta_k^*s_k^{*2} + C_{k9}s_k^*\theta_k^{*2} + C_{k10}s_k^{*3} \qquad 4.39$$

where $\theta_k^* = \theta_k - \bar{\theta}_k$, $s_k^* = s_k - \bar{s}_k$, and the C_{ki} are the coefficients determined by the fitting process; $\bar{\theta}_k$ and $\bar{s}_k$ are the mean values for the range of data to which the fit was made.

In diagnostic calculations it is more convenient to use an equation of state based on the in situ temperature. Table 1 summarizes the equation of state based on in situ temperature and salinity and used in diagnostic calculations in the Gulf of Mexico. The fit was made to one hundred pairs of T and S values at each level.

This type of approximation to the equation of state has been discussed by Bryan and Cox (1972). The approximation combines the computational efficiency associated with polynomials with the accuracy of the Knudsen-Ekman formula.

Table 1

Coefficients for the equation of state

depth (m)	ranges of T,S in fit $\bar{T}$	ΔT	$\bar{S}$	ΔS	C_{ki} i=1	2 X10^{1}	3 X10^{1}	4 X10^{3}	5 X10^{4}	6 X10^{3}	7 X10^{5}	8 X10^{5}	9 X10^{5}	10 X10^{5}
35.	23.50	17.00	35.75	3.50	24.53	-2.932	7.566	-3.987	3.590	-1.253	1.475	0.503	3.405	0.663
145.	18.50	13.00	36.25	1.50	26.77	-2.546	7.634	-4.202	3.562	-1.587	2.233	0.228	3.543	1.400
369.	13.00	13.00	35.75	2.50	28.66	-2.091	7.714	-4.602	3.232	-1.961	3.381	0.286	3.629	0.762
768.	6.50	4.00	35.00	1.00	31.06	-1.517	7.823	-5.269	2.989	-2.390	5.253	-0.695	3.882	-1.278
1369.	4.50	1.00	35.00	1.00	34.11	-1.442	7.827	-5.320	2.913	-2.466	6.488	2.351	6.571	7.879
2145.	4.50	1.00	35.00	1.00	37.64	-1.621	7.770	-4.984	3.053	-2.348	1.155	-0.810	8.744	2.240
3035.	4.50	1.00	35.00	1.00	41.62	-1.817	7.706	-4.597	3.070	-2.216	5.655	1.573	1.894	0.755

5. Computer Program

a. Program Structure

The program is a modification of a program written by Semtner (1974). The major changes were necessary in order to include "open boundaries" at the Straits of Florida and Yucatan and to improve the potential resolution of the model grid. Any future user of the program will, no doubt, have to make similar adaptions of his own. The program is written to be run on a UNIVAC 1108 computer.

The following discussion is essentially that of Semtner (1974). The appropriate changes have been included, usually without comment.

Figure 1 in section 4b shows the arrangement of grid points in a horizontal plane. The indices for θ, s, and Ψ points are J = 1,..., JMT for the north-south direction and I = 1,...,IMT for the east-west direction; the point J = 1, I = 1 is in the southwest corner. The indices for u and v points are J = 1,...,JMU and I = 1,...,IMU, where JMU = JMT-1 and IMU = IMT-1. The u,v point with the indices (J,I) is one-half grid spacing north and east of the θ,s point with the same indices. In the vertical direction the points are numbered by K = 1,...,KM with K = 1 for the surface layer.

The routine that controls the program is called MAIN. Here, the basic parameters for an experiment are either defined in arithmetic statements or read from cards. The coefficients associated with the geometry of the spherical coordinate system are computed here and then printed out.

Next the number of levels at each θ,s point is read from data cards. The routine then computes the number of levels at each

u, v point and the indices that define the northern and southern limits of the basin at each latitudinal line. All of the information is printed out.

MAIN will either start an experiment from scratch or restart an experiment already in progress. In either case, initial velocity, temperature, and salinity data are read in from a history tape and stored on the magnetic drum. These data will be used and updated during the course of an experiment.

Finally, MAIN steps forward the model integration by making calls to the subroutine STEP.

STEP begins each timestep by determining whether leapfrog or forward time differencing will be used. Then the data for longitudinal lines, I=1,2,3, and for two time-levels are brought into memory from the drum. The computation is then carried eastward, one longitudinal line at a time. STEP handles the data transfer within memory and between memory and drum so that longitudinal lines, I-1, I, and I+1 are available for the computations, while the data for line I+2 are being brought in for future use and the most recently computed data for line I-2 are being written out. The actual computations are accomplished by calls to CLINIC and TRACER which update the baroclinic velocity components and the temperature and salinity fields, respectively. If the experiment is diagnostic, STEP bypasses the call to TRACER. After these calculations are done for all the longitudinal lines the stream function is updated by a call to RELAX.

Finally, STEP attends to the print out of miscellaneous data and the writing of a history tape at specified intervals.

A listing of this program as used at the Atlantic Oceanographic and Meteorological Laboratories is available on request. The program is written in FORTRAN V.

b. Organization of Program Data

The data within the program are organized into "slabs". Each slab contains all of the data for a single longitudinal line. These data include arrays of temperature, salinity and the two baroclinic velocity components as well as miscellaneous boundary data. Each array is doubly dimensioned by the number of grid points in the north-south direction and the number grid points in the vertical direction. At any time the computation requires data at three time levels. Therefore, the model has three times as many slabs as there are longitude lines in the computational grid.

If all of the slabs are held in the memory of the computer at once, the size of the computational grid will be severly limited. For example, a model of the Gulf of Mexico with a grid dimensioned 24x16x7 would require over 50,000 words of memory and yet it would have a resolution of only 3/4 degree.

The memory requirement of this model is reduced by keeping only a few slabs in memory at one time. While the computation is proceeding, the slab which is needed next is being read into a memory buffer from the drum and the slab which has been most recently updated is being written out. These transfers are actually overlapped with the

computations. In this way the time lost while waiting for data transfers to be completed is kept to a minimum.

Althgether the model requires that eleven slabs be held in memory at once. They include slabs at three different time levels and five different longitude lines. Two of the slabs are input buffers and one is an output buffer.

The memory requirement of the the model is given by

$$JMT*(4*IMT + 62*KM + 93) + 19*JMT + 10*KM + 8000 \text{ words},$$

where IMT, JMT, and KM are the number of grid points in the east-west, north-south, and vertical directions respectively. Thus, a computer with a maximum of 50,000 words of memory can accomodate a model with a grid dimensioned by 72X48X7. In the Gulf of Mexico this would allow a resolution of 1/4 degree.

c. Treatment of Open Boundaries

Although the correct boundary conditions at open boundaries have been known for some time for barotropic models (Charney, Fjørtoft, and von Neumann, 1950), the problem remains unsolved for fully three dimensional baroclinic models.

At the open boundaries in the Gulf of Mexico model the baroclinic component of velocity is governed only by the condition that its derivative normal to the plane of the boundary vanishes. The transport stream function is specified everywhere along the boundary. Although it cannot be proved that these boundary conditions are correct, there are precedents for their use.

Holland and Hirschman (1972) used the same open boundary conditions

in their diagnostic study of the circulation of the North Atlantic Ocean. Cox (1970) also used these conditions in his Indian Ocean model. In both cases, the open boundary was the long southern edge of the model ocean. The transport across the open boundary was either very small as in the Holland and Hirschman model or actually set to zero as in the Cox model. Thus, while precedents exist they differ in important respects from the Gulf model where the open boundaries are narrow and the transport across them is great (30×10^6 m^3 sec^{-1}).

In order to prevent possible spurious effects due to the open boundaries from entering the model interior, the Straits of Yucatan and Florida are elongated into channels. The open boundary conditions are then applied at the outermost ends of the channels. The channels are necessary because features such as a strong anomalous upwelling appear near the open boundaries. The channels are successful in the sense that these anomalous features are confined to within a few grid points of the boundaries.

Some further considerations with regard to open boundaries are found in Section 6.

d. Data Requirements

To begin an experiment a number of parameters must be specified. The horizontal and vertical grid intervals must be set at the start of the routine MAIN. The dimensions of the arrays in all of the routines must be correctly set.

A set of data cards are used to specify the following parameters needed to run an experiment.

1) Control parameters: These parameters determine such factors as the starting and stopping points of the experiment, and the frequency with which data is written on the history tape.

2) The Timestep Interval: The standard guideline used in a timestep selection is that the grid interval divided by the timestep interval should be greater than both the speed of the fastest current, and the phase speed of the fastest wave present in the model (Courant, Friedrich, and Levy, 1928).

3) The Eddy Coefficients for Viscosity and Diffusion: Actual ocean observations suggest values for the horizontal coefficient of eddy viscosity ranging from 10^6 cm^2 sec^{-1} for small currents to $10^{10} cm^2$ sec^{-1} for the Antarctic Circumpolar Current (Fofonoff, 1962b). Typical values for this coefficient in large three dimensional models will range between 10^7 cm^2 sec^{-1} and 10^9 cm^2 sec^{-1}. The value depends on the resolution of the model; a coarser resolution requires a larger coefficient. Table 2 shows the eddy coefficients used in Cox's (1970)

Table 2.

Coefficients for Eddy Viscosity and Diffusion from Cox's (1970) Indian Ocean Model

Resolution	4° square	2° square	1° square
$A_m (cm^2/sec)$	$2x10^9$	$2x10^8$	$5x10^7$
$A_h (cm^2/sec)$	10^8	10^8	$5x10^7$
A_v & $\eta (cm^2/sec)$	1	1	1

Am = horizontal viscosity coefficient
A_H = horizontal diffusion coefficient
Av = vertical viscosity coefficient
η = vertical diffusion coefficient

Indian Ocean model; note that the size of the horizontal coeficients decrease by more than an order of magnitude as the resolution improves. The value of 1 cm^2 sec^{-1} for the vertical eddy coeficients shown in the table is comparable to the value predicted by thermohaline circulation theory (Veronis, 1969). The effects of different eddy viscosity coefficients in diagnostic experiments using the Gulf of Mexico model are discussed in the section on test results.

4) The Transport Stream Function at the Straits of Yucatan and Florida: The value of the stream function must be given for each point along the open boundaries. The only constraint on the specification is that the total volume transport into the model is matched by the total transport out.

5) The Bathymetry: The number of vertical levels at each temperature and salinity point must be specified. The bathymetry enters the model only in this discrete form.

In addition to the information on the data cards the program requires a history tape which holds an initial data file specifying the temperature and salinity at every grid point. The data file also specifies the wind stress and the surface boundary conditions for temperature and salinity.

The type of temperature data used in the model requires some comment. As was seen in Section 2 the equation for the conservation of thermal energy is correctly expressed in terms of the potential temperature, not the in situ temperature. Thus, to be consistent the model calculations should be done using potential temperature. In fact, however, the difference between potential temperature and in situ

temperature is slight (about 7% at 3000 meters), and would probably not be important in most calculations (Bryan, 1975). Furthermore, the question is only relevant to fully predictive experiments since in diagnostic experiments the temperature field is held fixed and an equation of state which is a function of in situ temperatures can readily be constructed.

The scale analysis in Section 2b shows that the pressure gradient force is a dominant term in the equations of motion. The pressure gradient force is determined, in part, by the distribution of density. The density field, in turn, is determined by the distribution of temperature and salinity. Therefore, it is clear that the temperature and salinity fields used in diagnostic experiments must be prepared carefully. A description of how the data was prepared for use in the Gulf of Mexico model can be found in the accompanying report, Model Studies of the Currents in the Gulf of Mexico.

e. Output

The history tape which is used to initialize the data fields for a given experiment is also used to record the time evolution of the experiment. If the experiment continues until a steady state is achieved, then the last file on the history tape represents the solution to the calculation.

In order to facilitate the interpretation of the data generated in the model a program has been written to produce a variety of illustrations. At the option of the user the program will draw contour plots of the bathymetry, the transport streamfunction, and the fields of temperature,

salinity, and the horizontal velocity components. In addition to these fields which are stored directly on tape, the program will also contour fields which are computed from the stored fields. These include the vertical velocity field, the pressure field, and the vertical component of relative vorticity. All of these contour plots are available in plan view and where appropriate at each vertical level. Contour plots of the velocity, temperature, and salinity fields are also available for vertical sections running either east and west or north and south. In all plots the appropriate topography is included. The user may specify that all or any portion of a field be contoured. He may also specify the contouring interval or allow the program to select it automatically. Finally, the program will also prepare vector plots for velocity and for the surface wind stress. Here arrows are drawn with lengths proportional to the magnitude of the velocity and directions parallel to the flow. All options available in contour plotting are similarly available in vector plotting.

A listing of this program is available on request. It is written in Fortran V and designed for use with a Gould 4800 plotting system.

6. Test Results

A number of tests have been conducted to determine the sensitivity of the model to variations in the experimental conditions.

All of the tests were based on the same set of temperature and salinity data. In particular, the data were the annual averages over one degree squares of all the temperature and salinity observations in the NODC raw data file. The data were interpolated onto the model grid

using quadratic splines in both vertical and horizontal directions. A few obviously bad points were removed by hand, and all the data at each level were smoothed once by the following rule

$$\theta_p^{new} = \frac{1}{2}\theta_p^{old} + \frac{1}{8}\sum_{i=1}^{4}\theta_i^{old} \qquad 6.1$$

where the summation is over the four surrounding points in the horizontal plane. The wind stress data were based on the annual averages over three degree squares as compiled by Andrew Bakum of the Pacific Environmental Group of the National Marine Fishery Service, NOAA. The wind stress components were interpolated onto the surface points using quadratic splines.

All of the test calculations were done on a grid with seven vertical layers and a horizontal resolution of ½ degree of longitude and latitude. The layer thicknesses were 70, 151, 297, 500, 703, 849, and 930 meters from top to bottom. The maximum depth allowed by the grid was 3500 meters. The model bathymetry was based on the bathymetry shown in Figure 2. The boundary of the model Gulf is shown in Figure 3; the boundary approximates the thirty meter isobath. The overlap of the boundary with Cuba was necessary to avoid constricting the Straits of Florida to less than three velocity grid points. The computational channels, discussed in Section 5c, are shown extending southward from 21.5°N and eastward from 81.5°W.

In every case the timestep was 0.5 hours and the vertical coefficient of eddy viscosity was 1 $cm^2 sec^{-1}$. The parameters which

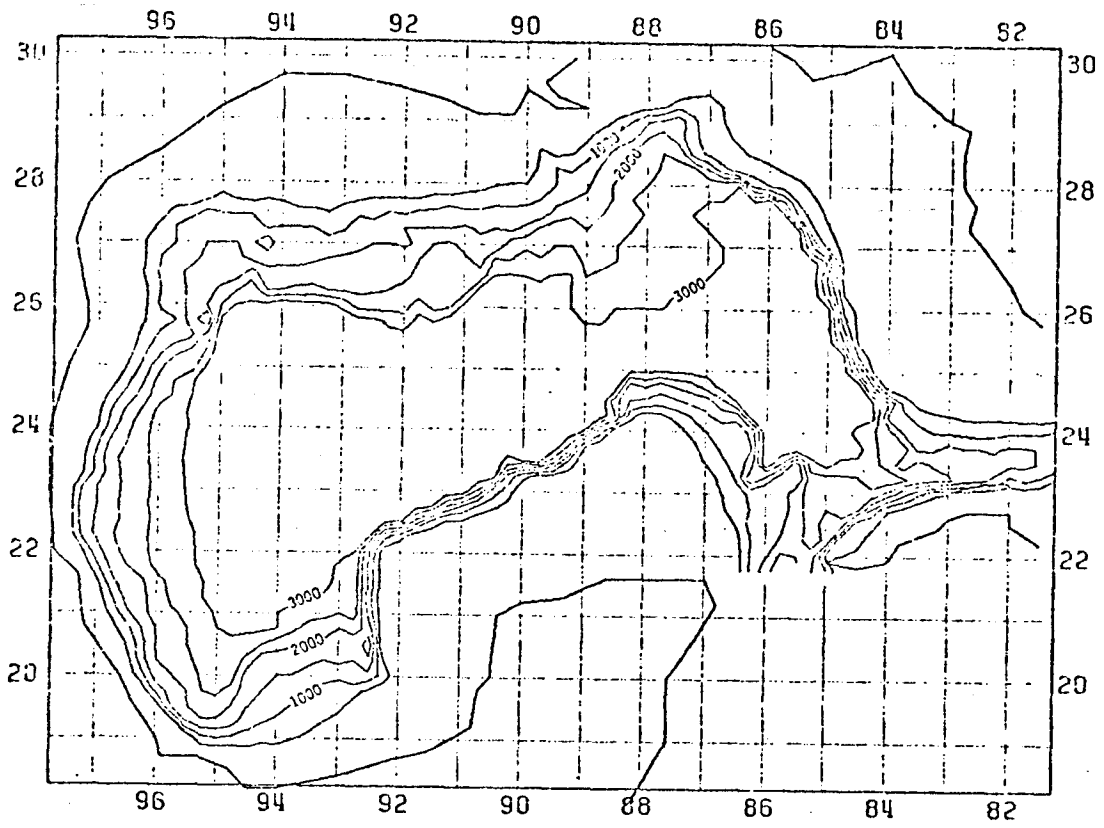

Figure 2. The bathymetry of the Gulf of Mexico. The contour interval is 500 meters.

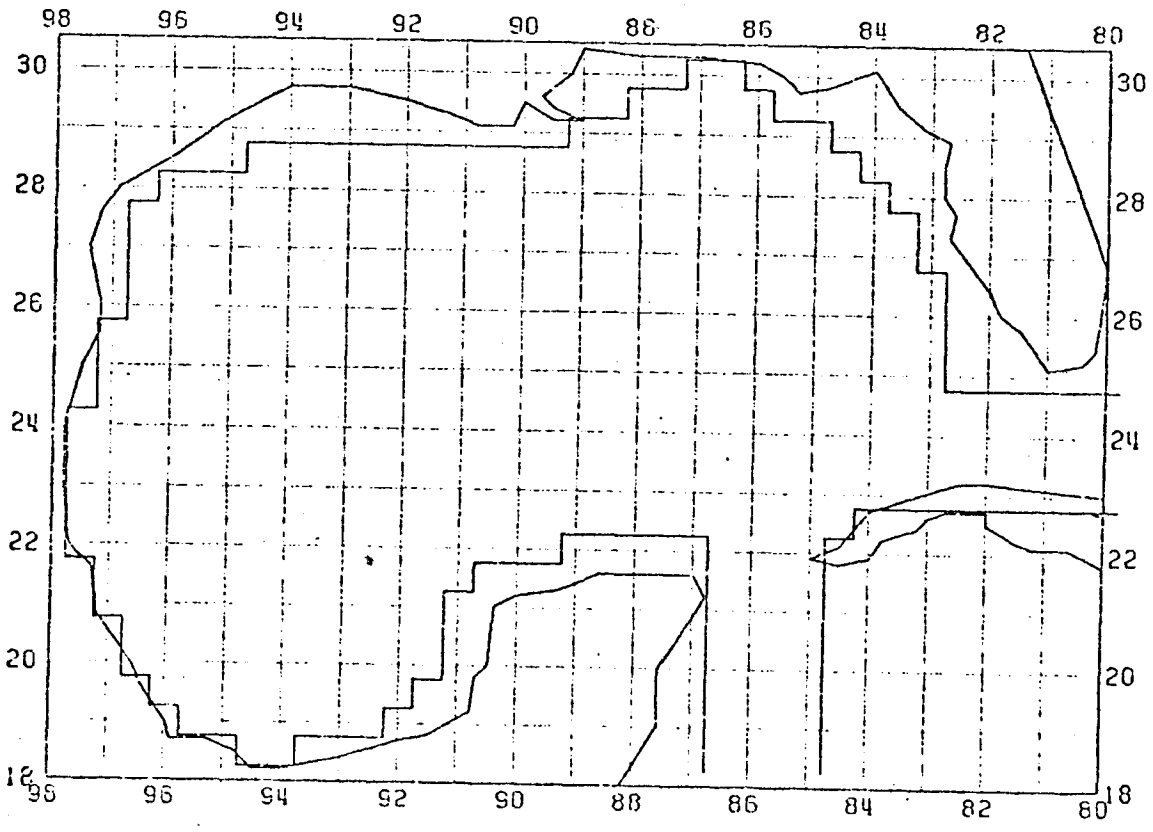

Figure 3. The model boundary superimposed on an outline of the Gulf of Mexico.

varied from test to test are shown in Table 3 and explained in detail below.

All of the tests (and, indeed all of the subsequent experiments) were energetically consistent. In every case a steady state was achieved in which the mean kinetic energy per unit volume changed less than 0.1% over the course of a time step.

Table 3.

Test	Transport $X10^6$ m^3/sec	Horizontal coefficient of viscosity cm^2sec^{-1}	Boundary Conditions	Wind Stress	Wide Shelf
T1	25	$2x10^7$	Zero gradient	yes	no
T2	25	$2x10^7$	geostrophic	yes	no
T3	25	$4x10^7$	Zero gradient	yes	no
T4	30	$4x10^7$	Zero gradient	yes	no
T5	25	$1x10^8$	Zero gradient	yes	no
T6	25	$2x10^7$	geostrophic	no	no
T7	30	$4x10^7$	Zero gradient	yes	yes

Figure 4 shows the typical evolution of an experiment in terms of the mean kinetic energy per unit volume.

a. Differences in Boundary Conditions.

Because of uncertainties in choosing the correct open boundary conditions (§5c), two distinct kinds of conditions were tested.

In Section 3c the horizontal velocity components (u, v), are partitioned into vertical averages, $(\overline{u},\overline{v})$, and deviations from the averages, $(\hat{u},\hat{v})$, such that

$$(u,v) = (\overline{u},\overline{v}) + (\hat{u},\hat{v}) \quad . \qquad 6.2$$

The standard boundary conditions for $\hat{u}$ and $\hat{v}$ at the entrance to the elongated Straits of Yucatan and the exit from the elongated Straits of Florida are

$$(\hat{u}_n,\hat{v}_n) = 0 \qquad 6.3$$

where the subscript, n, indicates the partial derivative in the direction normal to the plane of the boundary. In Table 3 these conditions are referred to as zero gradient boundary conditions.

The second kind of boundary condition specifies $\hat{u}$ and $\hat{v}$. The components are set by the thermal wind equation such that

$$f\hat{v}_z = - g\rho_x$$
$$\hat{u} = 0 \qquad 6.4$$

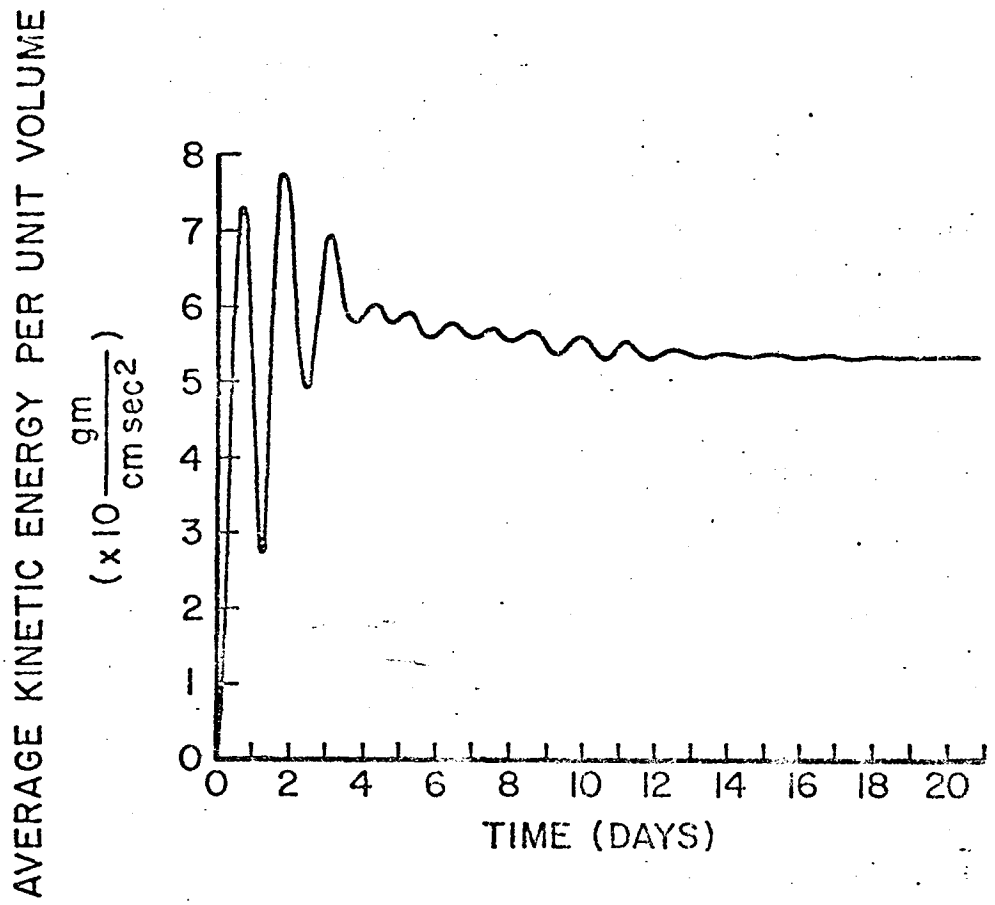

Figure 4. The variation of the mean kinetic energy per unit volume during the course of a typical experiment.

and

$$f\hat{u}_z = -g\rho_y$$
$$\hat{v} = 0 \qquad 6.5$$

Here, $f = 2\omega\sin\phi$ is the Coriolis parameter, g is the gravitational acceleration, and ρ is the density determined by the temperature and salinity data. In addition, a special viscosity is applied in the immediate vicinity of the open boundaries to damp away any computational noise which may arise there. Thus, extra terms are added to the right hand side of the momentum equations 3.3 and 3.4; the terms have the form $\nu(u^b-u)$ and $\nu(v^b-v)$, respectively, where the superscript indicates a boundary value. The form of ν is

$$\nu = \alpha \exp\{-\sinh(\sinh(r/r_o))\} \qquad 6.6$$

where r is the distance from the boundary, $\alpha = 10^{-4}\text{sec}^{-1}$, and $r_o = 150$ km; r_o is chosen so that ν vanishes within a distance less than the length of the computational channel. These boundary conditions are referred to as geostrophic in Table 2.

The effects of the different specifications can be seen by comparing test experiments T1 (zero gradient) and T2 (geostrophic). Figures 5a and 5b show the horizontal velocity vectors for the surface layers of T1 and T2, respectively. There are only minor differences. The results suggest that either kind of boundary condition is adequate. The zero gradient condition was decided upon because it is simpler to apply and it has precedents (§5c).

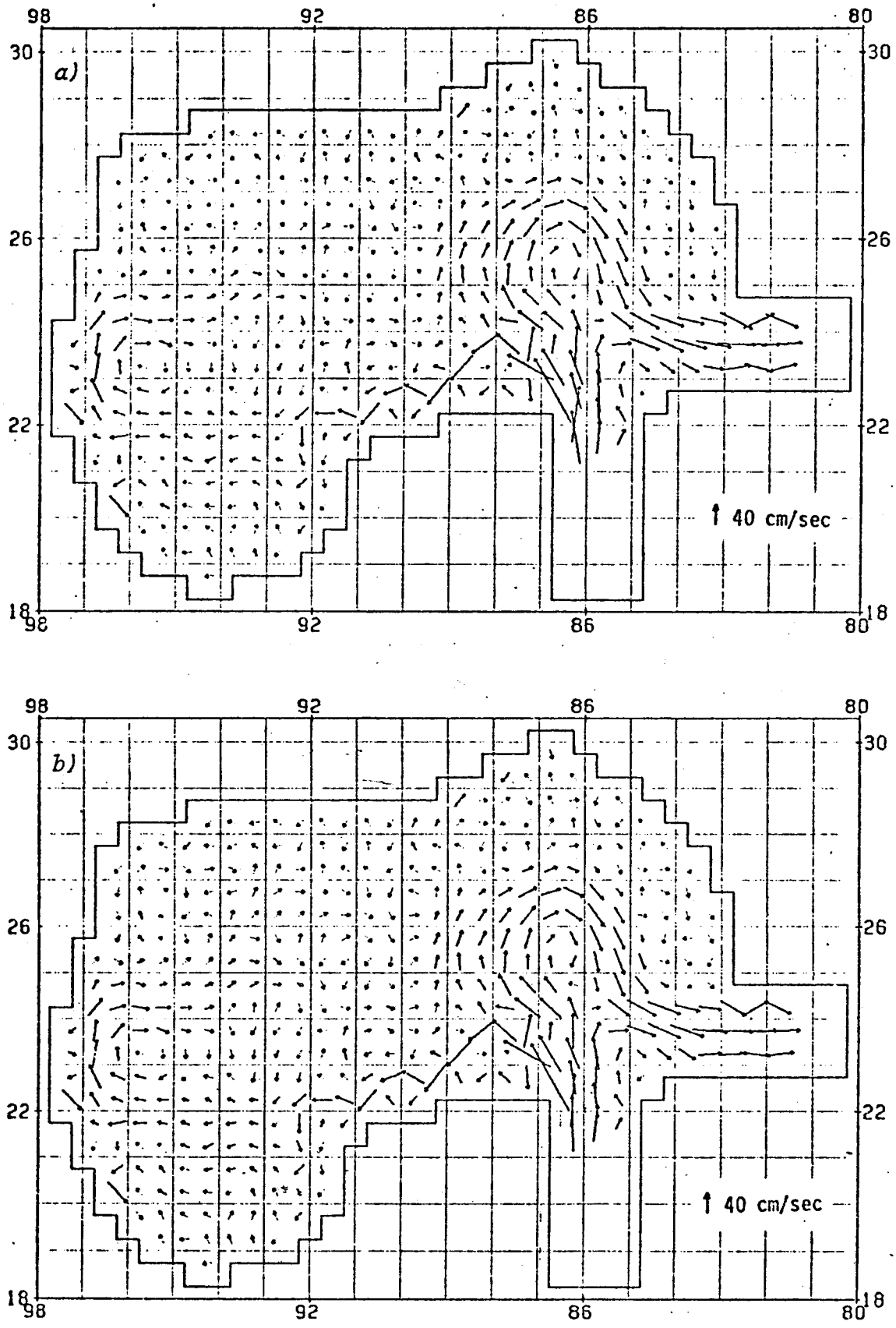

Figure 5. The velocity vectors in the surface layer at a depth of 35 meters for a) experiment T1 and b) experiment T2.

b. Differences in Transport through the Straits

Experiment T3 has a transport of $25X10^6$ m^3/sec through the Straits of Yucatan and Florida. Experiment T4 has been run under identical conditions except that the transport through the Straits is specified at $30X10^6$ m^3/sec. Figures 6a and 6b show the transport streamlines for experiments T3 and T4, respectively. In the western Gulf the streamline patterns are essentially the same and in the eastern Gulf they are remarkably similar. Assume that the correct transport through the Straits is $30X10^6$ m^3/sec. Then a comparison of Figures 6a and 6b shows that the main effect of under-specifying the transport by 17% is to cause a recirculation of water within the Loop Current and a westward flow of water along the northwestern coast of Cuba. Away from the Cuban coast the circulation is affected only slightly.

This result leads us to believe that small errors in the transport specified at the open boundary will not radically affect the interior circulation in a diagnostic experiment.

c. Experiments with and without Wind Stress

This section examines the importance of variations in the remaining boundary condition: the wind stress at the sea surface. First, an experiment, T1, was run using the wind stress field shown in Figure 7. Then a second calculation, T6, was made using the same conditions except that the wind stress was set to zero. Figures 8a and 8b show the streamline patterns from T1 and T6, respectively.

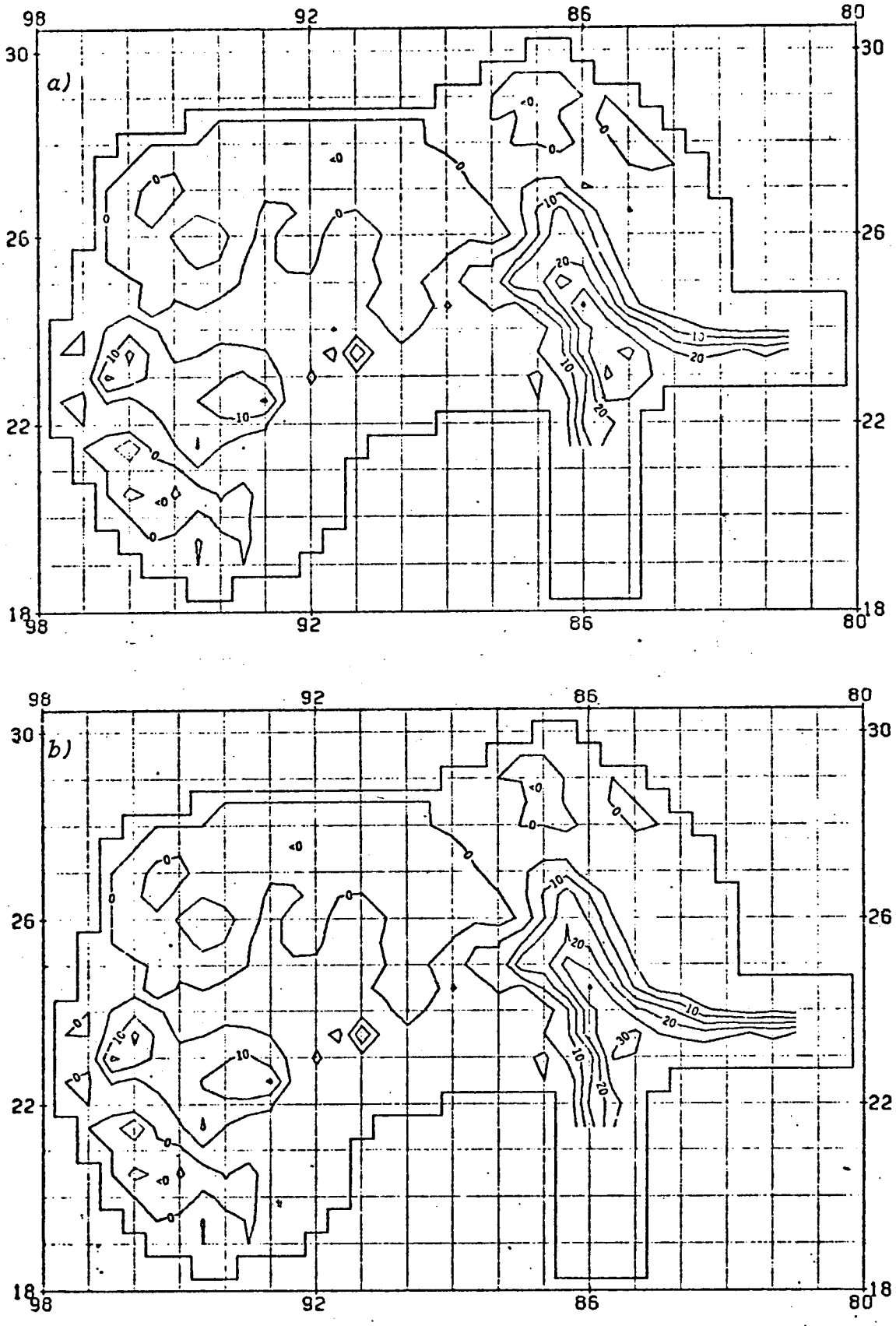

Figure 6. The transport streamlines for a) experiment T3 and b) experiment T4. The contour interval is $5X10^6$ $m^3 sec^{-1}$.

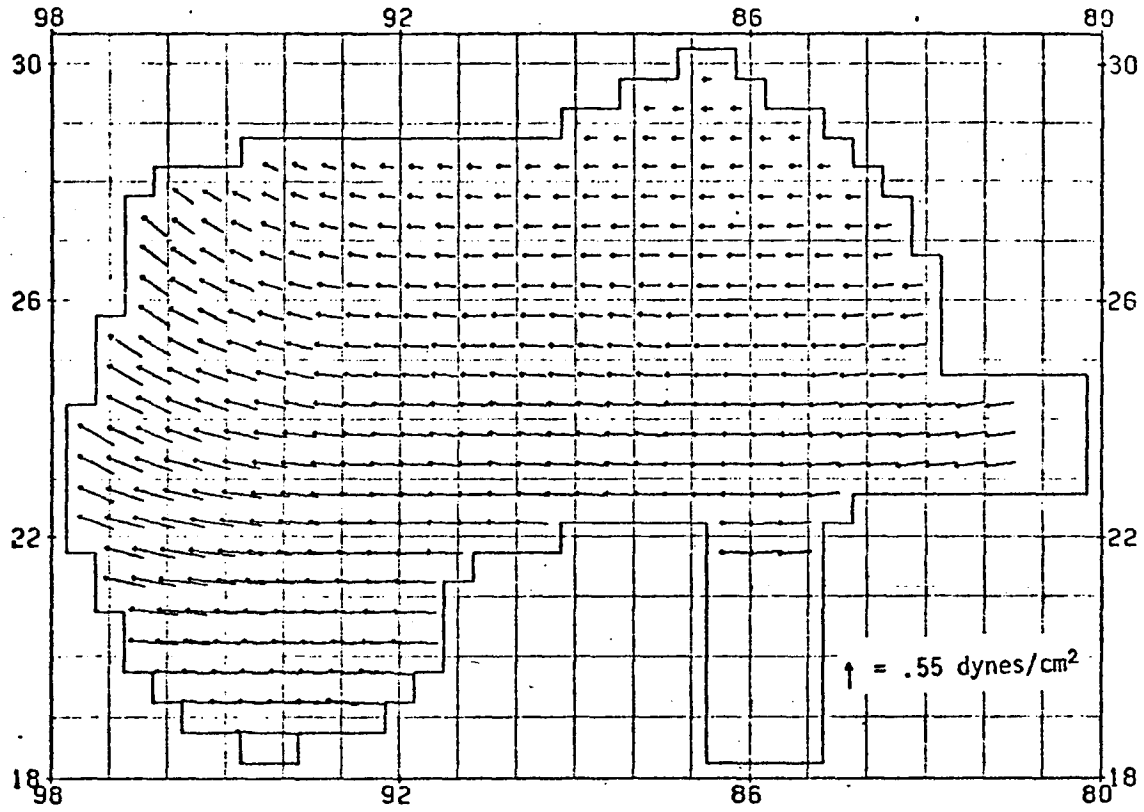

Figure 7. The annual average wind stress.

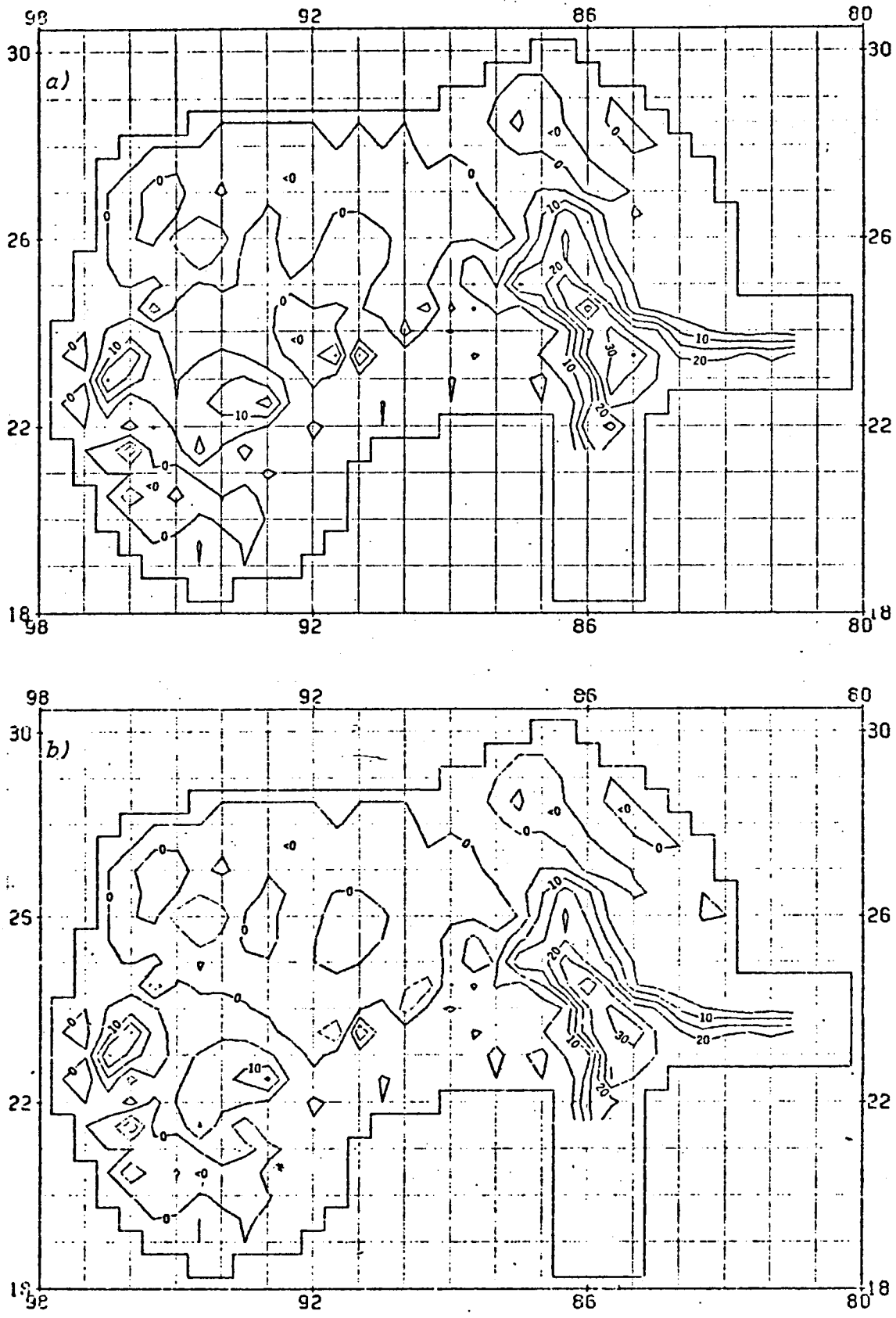

Figure 8. Same as Figure 6 except for a) experiment T1 and b) experiment T6.

There is a close similarity between the two pictures. The differences are mainly in regions where the circulation is weakest. (It should be remembered that in areas of weak circulation the streamfunction field is relatively flat. Thus, small changes in the choice of a contour can cause the patterns in Figures 8a and 8b to be more or less comparable.) The differences in the velocities for the surface layer (Figures 9a and 9b) and the deeper layers (not shown) are also negligible. There are small differences in the current on the Campeche Bank where the wind stress has caused some enhancement in the flow in experiment T1.

The negligible effect of the wind stress field on the circulation in these calculations agrees with the results of Holland and Hirschman (1972) for their diagnostic calculations of the circulation in the North Atlantic Ocean. The reason for this result is considered in the discussion concluding this section.

d. Differences in Viscosity

In Section 1, the results of two studies (Bryan, 1963 and Veronis, 1966) were quoted to the effect that the strength of the currents in a circulation model was ultimately determined by the amount of viscosity in the model. It is important, therefore, to test the sensitivity of the model in this regard. The horizontal coefficient of eddy viscosity must be large enough so that the frictional boundary layer is resolved by the grid; the width of this boundary layer is given by $2(Am/\beta)^{1/3}$ where $\beta = (2\omega\cos\phi/a)$ and a is the radius of the earth (Munk, 1950). Experiment T2 was run with an eddy coefficient sufficiently small so

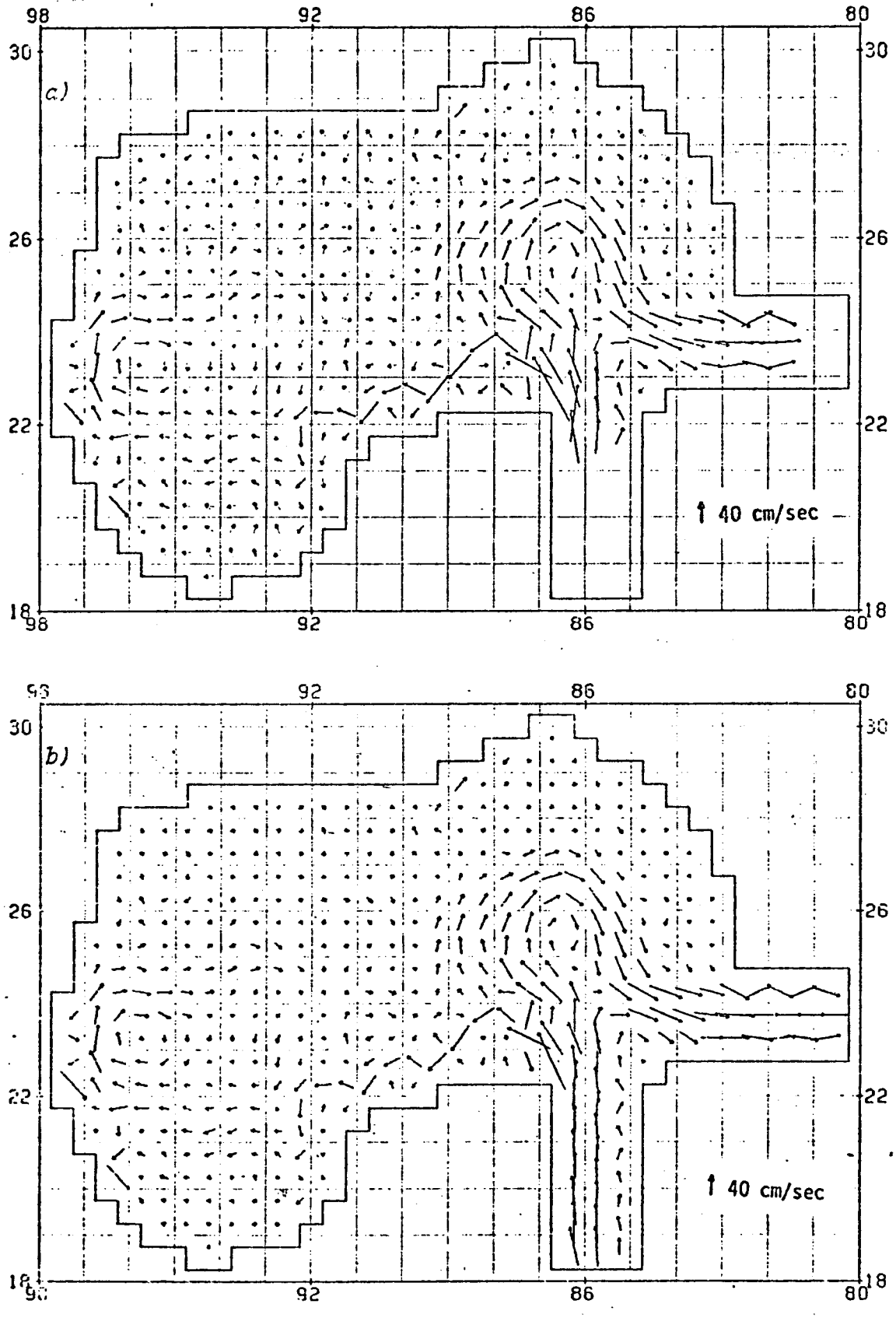

Figure 9. Same as Figure 5 except for a) experiment T1 and b) experiment T6.

that the frictional boundary layer was barely resolved. Two more experiments, T3 and T5, were run with larger coefficients.

Table 4 lists some of the parameters and results from the experiment, It can be seen that increasing the viscosity by a factor of 5 reduces the transport in the central western gyre by 35% and the transport in the Loop Current by 28%. The mean kinetic energy is decreased by 29%.

Figures 10a, 10b, and 10c show the streamlines for T2, T3, and T5, respectively. Experiment T2 shows a considerable amount of noise on the scale of the grid spacing. In experiment T3, the noise is greatly reduced, and in T5, it is essentially gone. On the other hand, all of the large scale features appear in each experiment. The

Table 4.

Results from Experiments with Varying Viscosity

	Am cm^2sec^{-1}	$2(A_m/\beta)^{1/3}$ Km	B $10^{12}m^2/sec$	C $10^{12}m^2/sec$	D $gm/cm\ sec^2$
T2	$2x10^7$	90	20	36	45
T3	$4x10^7$	120	16	32	38
T5	10^8	160	13	26	32

Am=Horizontal coefficient eddy viscosity

$2(Am/\beta)^{1/3}$= Width of the frictional boundary layer

B = Maximum transport in the central western gyre

C = Maximum transport in the Loop Current

D = Mean kinetic energy per unit volume

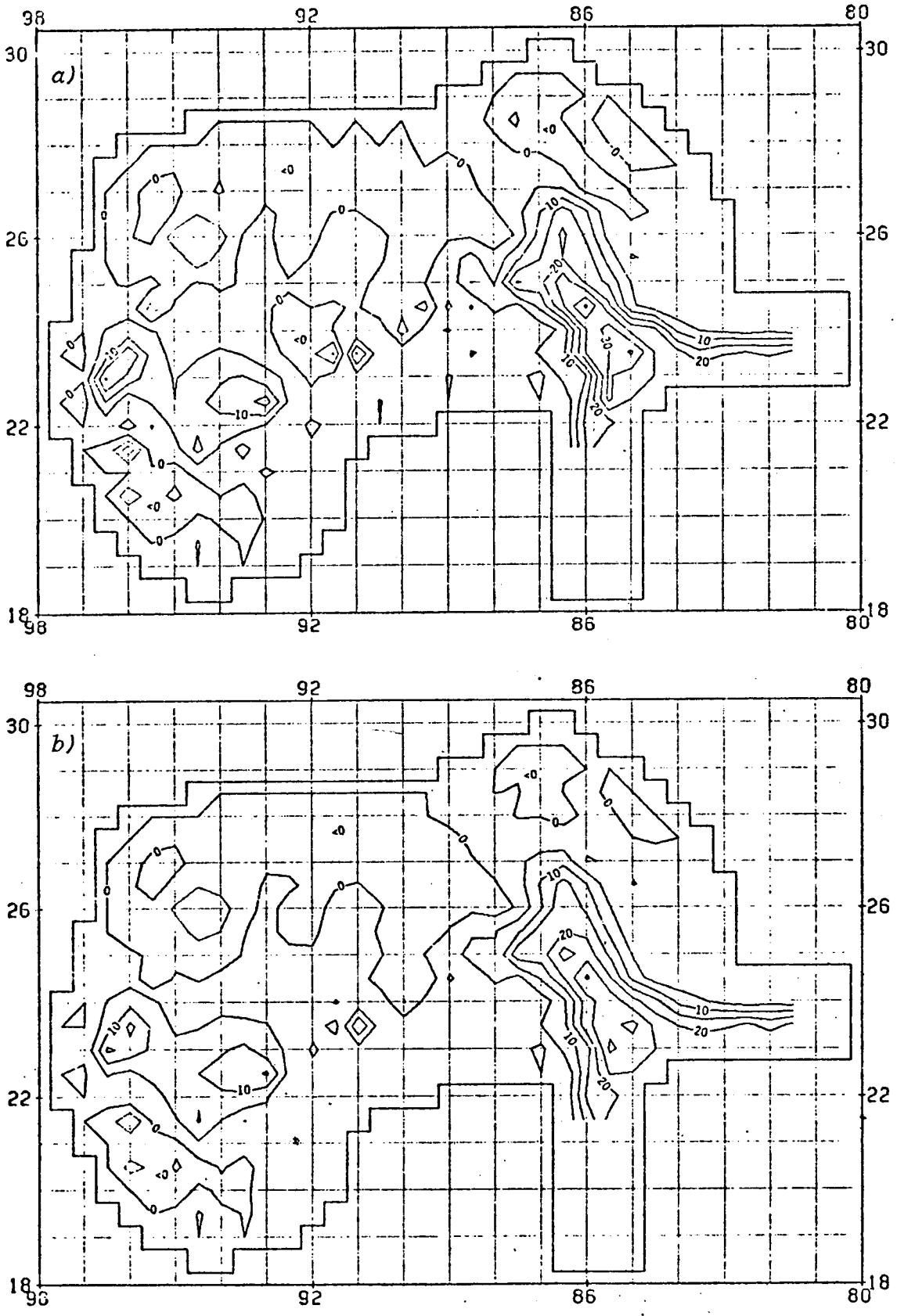

Figure 10. Same as for Figure 6 except for a) experiment T2 and b) experiment T3.

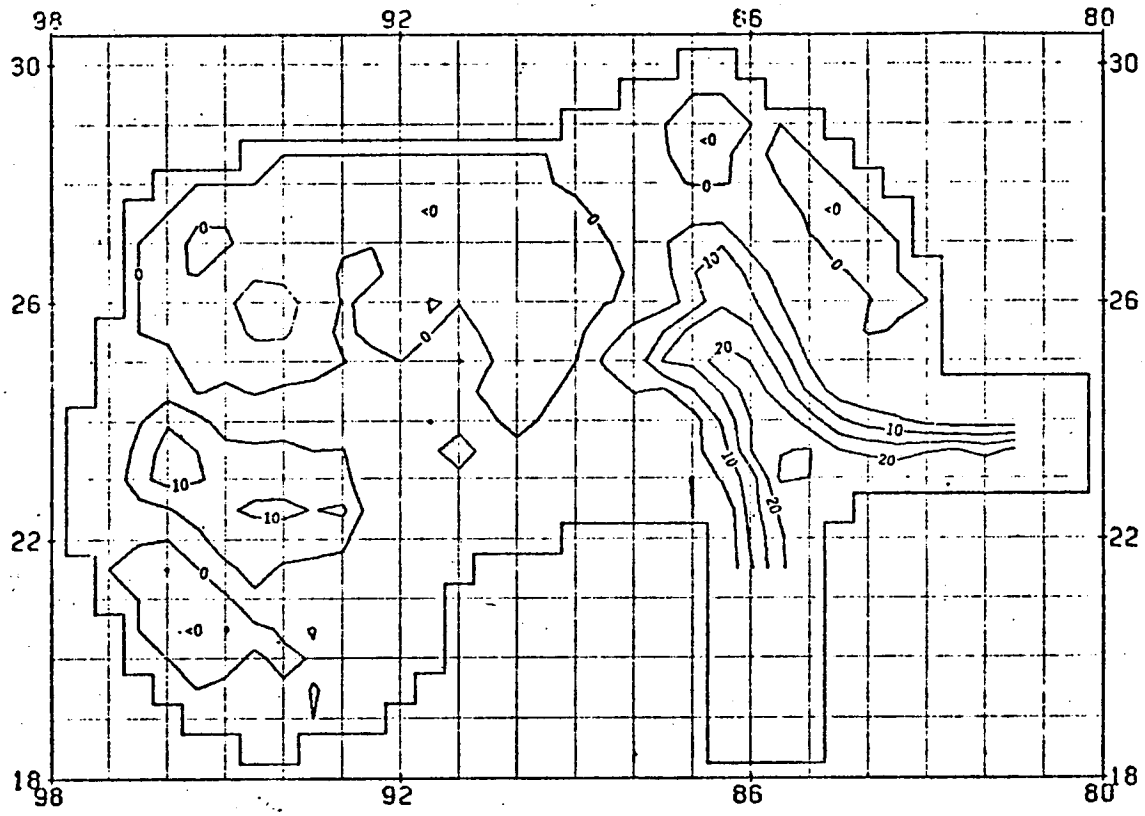

Figure 10c. Same as Figure 6 except for experiment T5.

effect of increasing viscosity is clearly evident on the Loop Current. In addition to becoming smoother, the Loop broadens and the stream function gradients become smaller. Since the vertically averaged velocity is proportional to the gradient of the stream function, the more widely spaced streamlines are associated with lower velocities.

On the basis of these results the compromise value of $A_m = 4 \times 10^7$ cm^2/sec was chosen for subsequent experiments.

e. Effect of Extending the Shallow Shelves

The extensive shelves in the Gulf of Mexico represent a serious difficulty for the model. In the present model the thickness of the topmost layer in the standard grid is 70 meters. This layer extends horizontally inshore as far as the 35 meter isobath. As seen in Figure 3, the standard grid excludes a fair sized portion of the shelf waters. In order to resolve these areas more efficiently one or more additional thin layers would have to be added to the top of the model. This would increase the size of the grid and, therefore, decrease the possible horizontal resolution of the model.

In order to explore a simpler alternative, an experiment was performed on a grid in which the top layer had been extended shoreward to the 15 meter isobath. The results of this experiment, T7, can be compared with those of experiment T4, done on the standard grid. Although, the expanded grid only has about one additional row of grid points around the edge, the difference between the two experiments is striking (Figures 11a and 11b). On the expanded grid, a vigorous current has appeared flowing from the Mississippi Delta

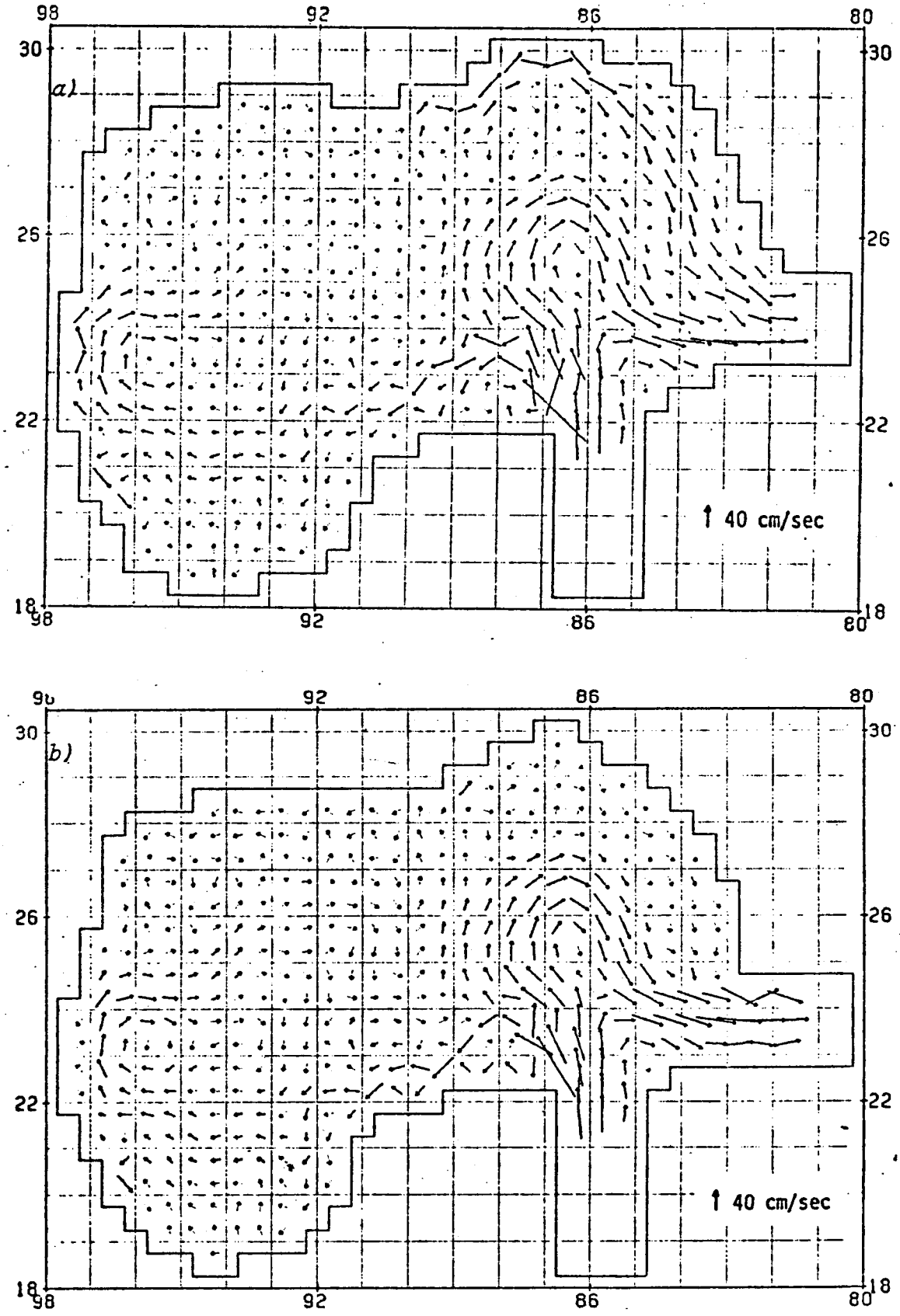

Figure 11. Same as Figure 5 except for a)experiment T7 and b) experiment T4.

southward across the west Florida Shelf, in place of the much weaker southward flow in experiment T4. Such a strong current, with velocities as large as those in the Loop Current, is not realistic. The reasons for its appearance are not known. The shallow shelf is already quite wide in the standard grid, and it is difficult to imagine why the addition of one more row of points should have such a drastic effect.

In both experiments there are strong currents along the Campeche Bank west of 88° W longitude. The current speeds here are also probably too large. On the other hand, the current direction is consistent with the interior flow and the currents are probably correct in this sense.

As a result of this test the expanded grid was rejected. Also in response to this test a small amount of bottom friction was added to the model. Wherever the grid is only one layer thick a bottom stress is applied. It has the form

$$\tau_b^\lambda = \gamma u \qquad 6.7$$

$$\tau_b^\phi = \gamma v$$

where u and v are the zonal and meridional components of velocity, τ_b^λ and τ_b^ϕ are the corresponding bottom stresses, and $\gamma = 7X10^{-8}$ sec^{-1} is the constant coefficient of proportionality.

f. Discussion

Perhaps the most important results of the test experiments were those which showed that large changes in the applied wind stress

and in the transport through the Straits of Yucatan and Florida had relatively little effect on the circulation in the interior of the basin. These results suggest that observational uncertainties leading to errors in these boundary conditions will not destroy the value of a diagnostic experiment. It is interesting to speculate about why this is so.

To begin, it is convenient to refer to the vorticity equation for the transport streamfunction, the equation which governs the vertically averaged flow in the model. Equation 3.22 can be written in the form:

$$\nabla_H^2 \Psi_t = -\frac{m}{a^2}(2\omega n)_\phi \Psi_\lambda - \frac{m}{a}\{(\frac{\tau^\lambda}{m})_\phi - (\tau^\phi)_\lambda\} + \frac{m}{a^2}\{(p_b)_\lambda h_\phi - (p_b)_\phi h_\lambda\} + \frac{m}{a^2}\{G_\lambda^\phi - (\frac{G^\lambda}{m})_\phi\} \qquad 6.8$$

where τ^λ, τ^ϕ = components of wind stress,

and p_b = pressure at the bottom. (The bottom refers not only to the deepest parts of the basin, but to the entire ocean-earth interface.)

The remaining quantities are defined in Section 3a. The terms on the right hand side represent in order the so-called planetary vorticity tendency, the curl of the wind stress, the bottom pressure torque, and the combined effects of non-linearities and lateral viscosity. The wind stess appears explicitly in equation 6.8; the transport through open boundaries enters the solution to equation 6.8 through the boundary condition on Ψ.

Traditionally, circulation theory argues that in the interior of the ocean basins lateral friction and non-linear effects are not important, and that,therefore,the last term in equation 6,8 can be neglected. Then, if either the depth or the bottom pressure is constant, the third term on the right in equation 6.8 vanishes, and for steady flow the planetary vorticity tendency is balanced by the curl of the wind stress (Sverdrup, 1947). In other words, when the pressure gradient goes to zero at some level above the bottom, the transport in the ocean interior is completely determined by the wind stress. However, if the depth and the bottom pressure are variable, then the bottom pressure torque term remains and it may be important. In fact, Holland and Hirschman (1972) have found the bottom pressure torque to be the most important determinant of the transport in their diagnostic model of the North Atlantic Ocean.

In order to show that the bottom pressure torque is important in the Gulf of Mexico model it must first be shown that the nonlinear and frictional effects are negligible in the interior of the basin. By an extension of the scaling arguments in Section 2b it can be shown that, relative to the planetary vorticity term in equation 6.8, the non-linear and frictional effects are scaled by the Rossby Number for the vertically averaged flow and the Horizontal Ekman Number, respectively. In the interior the largest vertically averaged velocities in the Loop Current do not exceed 50 cm/sec and the length scale over which the flow varies is about 100 km. Using these

values and the value of $4X10^7$ cm^2/sec for the horizontal coefficient of eddy viscosity the Rossby Number is $5X10^{-2}$, and the Ekman Number $4X10^{-3}$, both much less than unity. Thus, the last term in equation 6.8 may be neglected. If the flow is steady, then the remaining terms in the equation are the planetary vorticity tendency, the curl of the wind stress, and the the bottom pressure torque. In section 6c it was shown that removing the wind stress had only a slight effect on the model circulation (Figures 8a, 8b, 9a, and 9b). The result suggests that the interior balance is primarily between the planetary vorticity tendency and the bottom pressure torque. Finally, in section 6b it was demonstrated that a 17% reduction of the transport through the Straits of Yucatan and Florida caused significant changes in the transport only near the Cuban coast (Figures 6a and 6b). This suggests that the interior balance remains unchanged and the adjustment to the transport boundary condition occurs only in a narrow boundary layer along the Cuban coast.

The above discussion refers only to the dynamics of the model. It does not suggest that the wind stress and variations in the transport through the Straits are not important in the actual Gulf or in a fully predictive model of the Gulf.

References

Arakawa, Akio(1966) Computational design for long-term numerical integration of the equations of fluid motion: Two-dimensional incompressible flow. Part I. J. Comp. Phys., 1, 119-143.

Bryan, K. (1963) A numerical investigation of a nonlinear model of a wind-driven ocean. J. Atmos. Sci., 20, 594-606.

Bryan, K. (1969) A numerical method for the study of the circulation of the world ocean. J. Comp. Phys., 4, 347-376.

Bryan, K. (1975) Numerical Models of the Ocean Circulation. Three-dimensional Models of the Ocean Circulation. Washington, D.C.: National Academy of Sciences, 94-106.

Bryan, K., and M. D. Cox (1967) A numerical investigation of the oceanic general circulation. Tellus, 19,54-80.

Bryan, K., and M. D. Cox (1968) A nonlinear model of an ocean driven by wind and differential heating. Parts I and II. J. Atmos. Sci., 25, 945-978.

Bryan, K., and M. D. Cox (1972) An approximation to the equation of state for sea water, suitable for numerical ocean models. J. Phys. Oceanogr., 2, 514-517.

Carrier, G. F., and A. R. Robinson (1962) On the theory of the wind-driven ocean circulation. J. Fluid Mech., 12, 49-80.

Charney, Jule G. (1955) The Gulf Stream as an inertial boundary layer. Proc. Nat. Acad. Sci., Washington, D. C., 41, 731-740.

Charney, J. G., R. Fjortoft, and J. von Neumann (1950) Numerical integration of the barotropic vorticity equation. Tellus, 2, 237-254.

Courant, R., K. Friedrichs, and H. Levy (1928) U Bar Die Partiellen Differentialgleichungen der Mathematischen Physik. Math. Ann., 100, 32-74.

Cox, M. D. (1970) A mathematical model of the Indian Ocean. Deep-Sea Res., 17, 47-75.

Cox, M. D. (1975) Numerical Models of Ocean Circulation. A Baroclinic Numerical Model of the World Ocean: Preliminary Results. Washington, D. C.: National Academy of Sciences, 107-120.

Fofonoff, Nicholas P. (1962a) The sea, ideas and observations. Physical properties of sea-water. New York and London: Pergamon Press, Vol. 1, 3-30.

Fofonoff, Nicholas P. (1962b) The sea, ideas and observations. Dynamics of ocean currents. New York and London: Pergamon Press, Vol. 1, 323-396.

Forsyth, George Elmer and Wolfgang R. Wasow (1960) Finite-difference methods for partial difference equations. New York: Wiley, 444 pp.

Galt, J. A. (1975) Development of a simplified diagnostic model for interpretation of oceanographic data. NOAA TR ERL 339-PMEL, U. S. Dept. of Commerce.

Gill, A. E. (1971) Ocean models. Phil. Trans. R. Soc. Lond. A. 270, 391-413.

Gill, A. E., and K. Bryan (1971) Effects of geometry on the circulation of a three-dimensional southern-hemisphere ocean model. Deep-Sea Res., 18, 685-721.

Hendershott, Myrl, and Walter Munk (1970) Tides, Ann. Rev. Fl. Mech., 2, 205-224.

Holland, William R., and Alan D. Hirschman (1972) A numerical calculation of the circulation in the North Atlantic Ocean. J. Phys. Ocean., 2, 336-354.

Lamb, Horace (1932) Hydrodynamics. London: Cambridge University Press, 6th ed. 738 pp.

Leendertse, J. J. (1970) A water-quality simulation model for well-mixed estuaries and coastal seas. I. Principles of compilation. Memo RM-6230-RC. The Rand Corp., Santa Monica, Calif.

Monin, A. S., and A. M. Yaglom (1971) Statistical Fluid Mechanics. MIT Press, Cambridge, 769 pp.

Morgan, G. W. (1956) On the wind-driven ocean circulation. Tellus, 8, 301-320.

Munk, W. H. (1950) On the wind-driven ocean circulation. J. Meteoro., 7, 79-93.

Neumann, Gerhard and Willard J. Pierson, Jr. (1966) Principles of Physical Oceanography. Englewood Cliffs: Prentice-Hall, 545 pp.

Peng, Chich-Yuan, and Ya Hsueh (1974) A diagnostic calculation of continental shelf circulation, Dept. of Oceanography, Florida State University, Tallahassee, Florida.

Phillips, O, M. (1966) The dynamics of the upper ocean. Cambridge University Press, Cambridge, 261 pp.

Reid, Robert O., and Bernie R. Bodine (1968) A numerical model for storm surges in Galveston Bay. J. Waterways and Harbors Div., ASCE, 94, No. WWi, Proc. Paper 5805, 33-37.

Sarkisyan, A. S. (1966) Theory and computation of ocean currents. Gidrometeoizdat (English translation IPST Press, Jerusalem 1969).

Semtner, A. J., Jr. (1974) An oceanic general circulation model with bottom topography. Numerical simulation of weather and climate. Tech. Report No. 9, Univ. of Cal., Los Angeles, 99 pp.

Stommel, H. M. (1948) The westward intensification of wind-driven ocean currents. Trans. Amer. Geophys. Union, 29, 202-206.

Stommel, H. M. (1958) The abyssal circulation. Deep-Sea Res., 5, 80-82.

Stommel, H. M. (1965) The Gulf Stream. A physical and dynamical description. Berkeley: Univ. of Calif. Press. 248 pp.

Sturges, Wilton, and John P. Blaha (1976) A western boundary current in the Gulf of Mexico. Science, 192, 367-369.

Sverdrup, H. U. (1947) Wind-driven currents in a baroclinic ocean; with application to the equatorial currents of the eastern Pacific. Proc. Nat. Acad. Sci., Washington, D. C., 33, 310-326.

Veronis, George (1966) Wind-driven ocean circulation. Part 2. Numerical solutions of the non-linear problem. Deep-Sea Res., 13, 31-55.

Veronis, George (1969) On theoretical models of the thermocline circulation. Deep-Sea Res., 16 Suppl., 301-323.

Warren, B. A. (1971) Evidence for a deep western boundary current in the south Indian Ocean. Nature Phys. Sci., 229(1), 18-19.

Webster, F. (1965) Measurements of eddy fluxes of momentum in the surface layer of the Gulf Stream. Tellus, 17, 239-245.

The Department of the Interior Mission

As the Nation's principal conservation agency, the Department of the Interior has responsibility for most of our nationally owned public lands and natural resources. This includes fostering sound use of our land and water resources; protecting our fish, wildlife, and biological diversity; preserving the environmental and cultural values of our national parks and historical places; and providing for the enjoyment of life through outdoor recreation. The Department assesses our energy and mineral resources and works to ensure that their development is in the best interests of all our people by encouraging stewardship and citizen participation in their care. The Department also has a major responsibility for American Indian reservation communities and for people who live in island territories under U.S. administration.

The Minerals Management Service Mission

As a bureau of the Department of the Interior, the Minerals Management Service's (MMS) primary responsibilities are to manage the mineral resources located on the Nation's Outer Continental Shelf (OCS), collect revenue from the Federal OCS and onshore Federal and Indian lands, and distribute those revenues.

Moreover, in working to meet its responsibilities, the **Offshore Minerals Management Program** administers the OCS competitive leasing program and oversees the safe and environmentally sound exploration and production of our Nation's offshore natural gas, oil and other mineral resources. The MMS **Minerals Revenue Management** meets its responsibilities by ensuring the efficient, timely and accurate collection and disbursement of revenue from mineral leasing and production due to Indian tribes and allottees, States and the U.S. Treasury.

The MMS strives to fulfill its responsibilities through the general guiding principles of: (1) being responsive to the public's concerns and interests by maintaining a dialogue with all potentially affected parties and (2) carrying out its programs with an emphasis on working to enhance the quality of life for all Americans by lending MMS assistance and expertise to economic development and environmental protection.